A STUDY OF THE OPTICAL ABSORPTION AND PHOTOCONDUCTIVITY

OF GAMMA-IRRADIATED LiF

by

Charles Denton Marrs

B.S., Fort Hays Kansas State College, 1973

─────────────

A Master's Thesis

submitted in partial fulfillment of the
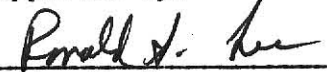
requirements for the degree

MASTER OF SCIENCE

Department of Physics

Kansas State University
Manhattan, Kansas

1976

Approved by:

Major Professor

TABLE OF CONTENTS

LIST OF FIGURES

ACKNOWLEDGEMENTS

I dedicate this work to my wife, Victoria, and my daughter, Diedra Lynn. Their love, patience and understanding provided the support so necessary for its completion.

I wish to thank my major professor, Ron Lee, and Fred Merklin for their guidance and encouragement in completing the work, for without them none of it would have been possible. I also wish to thank Milton Richter for his help in drawing the figures and Prochy Sethna for reading the manuscript.

Finally, I wish to thank the Physics Department for their financial support during completion of the work.

I. INTRODUCTION

The passage of ionizing radiation through an alkali halide produces a coloring of the crystal.[1,2,3] The production of color has been shown to result from the trapping of electrons and holes, released by radiation, at crystal imperfections and impurity sites. The defect centers formed by the trapped electrons and holes have excited states which allow the absorption of photons that are normally transmitted by the crystal. Such defect centers that give rise to optical absorption spectra are called "color centers."[4,5,6] The F center is the principal color center produced by ionizing radiation.[5,6,7,8]

In the band picture of solids, alkali halides are described by a filled valence band and an empty conduction band separated by a forbidden energy gap.[8,9,10,11] The ground and excited states of the F center are localized energy levels in the forbidden energy gap. The transition from the ground state to the first excited state on absorption of a photon gives rise to the F center's optical absorption band. Other color centers demonstrate the same behavior, thus several absorption bands, characteristic of the color centers, would be observed in an optical absorption measurement.[3,4,7,8,12]

The fact that there are trapped electrons and holes in the bandgap raises the possibility that the alkali halides could be photoconductive. Past work has shown several of the alkali halides exhibit photoconductivity generated by electrons and holes from defect centers and impurities.[3,8,13,14,15,16,17,18,19,20]

Recent work by Metha on the optical bleaching of absorption bands in LiF suggested that LiF could also be photoconductive.[21] Nelson studied the photoconductivity of LiF, at room temperature, in the spectral range from 400 nm to 200 nm and observed a photoconductivity peak at 278 nm.[22] It

1

was observed that this was the same region as a small absorption band that appeared as a shoulder on the long-wavelength side of the F center absorption band in LiF. At room temperature the F center absorption band appears at 250 nm.[3,4]

The objective of this research is to study the photoconductivity of gamma-irradiated LiF in the temperature range 85°K to 300°K and to study the optical absorption of the shoulder on the F center optical absorption band with plane-polarized light at 90°K and 300°K.

II. THEORY

A photoconductor in the broadest sense is defined as any material whose electrical conductivity can be changed by the absorption of photons.[9,23, 24] In this sense every semiconductor and insulator is a photoconductor.

Processes in a Photoconductor

The absorption of photons in a semiconductor or insulator is a quantum process in which electrons are raised from trapping sites or the valence band to the conduction band.[7,8,9,23,24,25] For the case of removing an electron from the valence band, a free hole is also produced. Under the influence of an applied electric field, the free electrons and free holes will move through the crystal lattice producing a current, initiated by the absorption of photons.

Figures 1, 2, and 3 show some of the electronic transitions found in a photoconductor.[19,23,25] These transitions can be divided into three types: 1) absorption and excitation, 2) trapping and capture, and 3) recombination.

There are four possible types of absorption and excitation transitions that result in photoconductivity, see Fig. 1. Transition 1 corresponds to absorption by the atoms of the crystal itself, producing a free electron and a free hole. Transition 2a corresponds to absorption at localized imperfections, producing a free electron and a hole bound in the neighborhood of the imperfection. Transition 2b is similar to 2a, but the difference is the electron is promoted to an excited state below the conduction band yet

3

FIGURE 1

Absorption and excitation processes in a photoconductor

THIS BOOK CONTAINS NUMEROUS PAGES WITH DIAGRAMS THAT ARE CROOKED COMPARED TO THE REST OF THE INFORMATION ON THE PAGE.

THIS IS AS RECEIVED FROM CUSTOMER.

Conduction Band

Valence Band

Heat

E_g

1

2a

2b

3

* — excited state

5
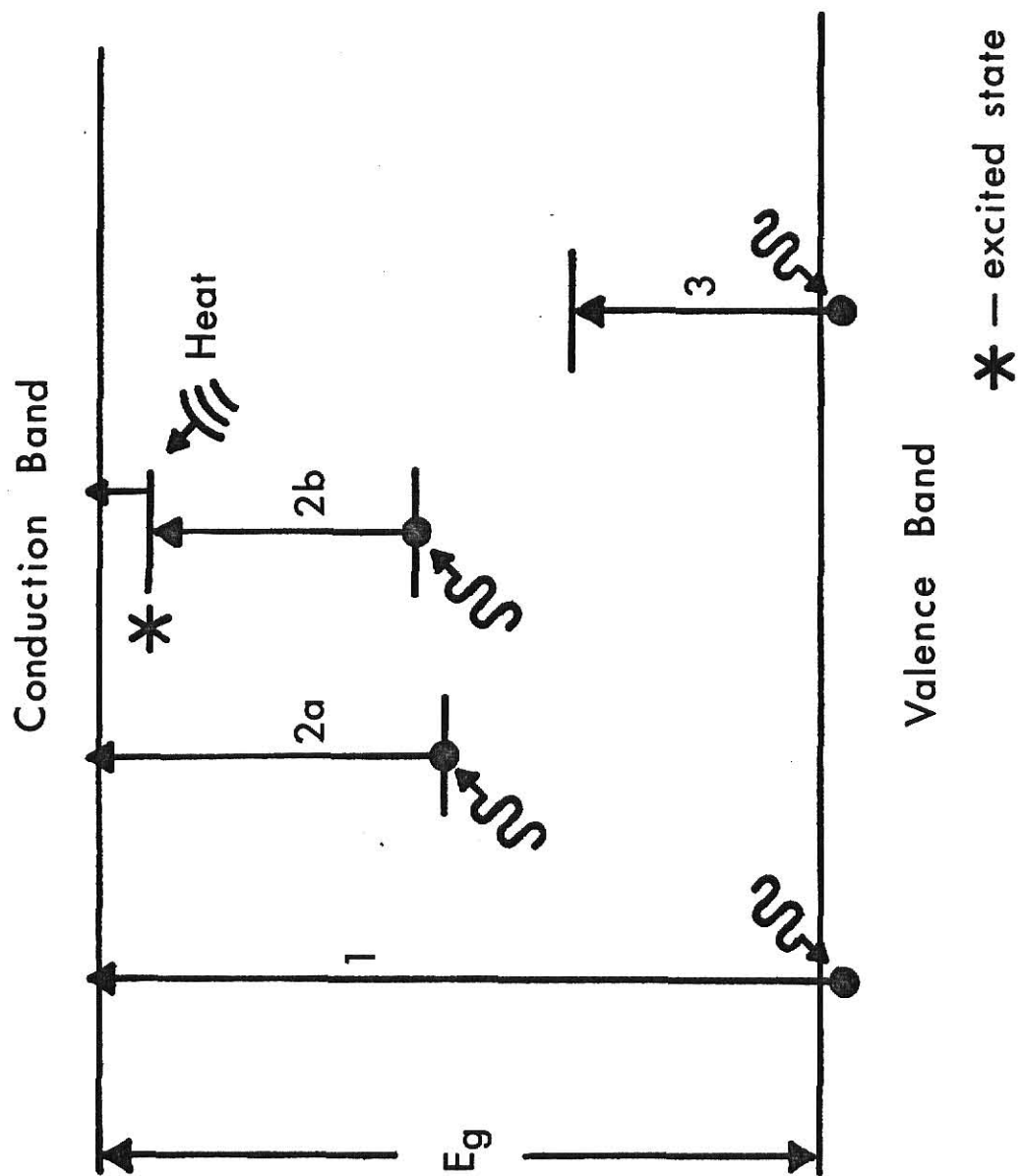
FIGURE 2

Trapping and capture processes in a photoconductor

Conduction Band

Heat

5'

5

7

Valence Band

6

Heat

4'

4

E_g
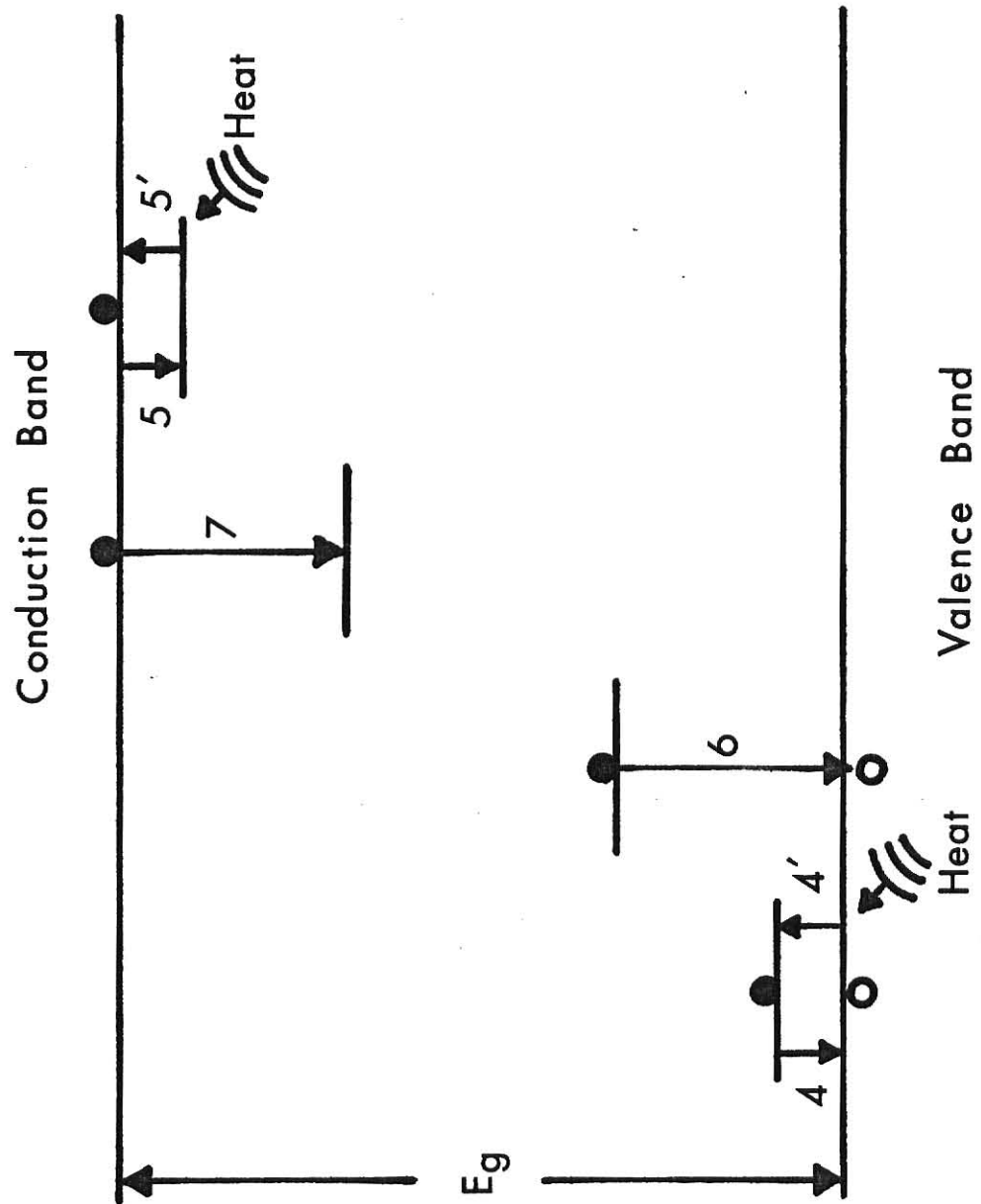
FIGURE 3

Recombination processes in a photoconductor

Conduction Band

Valence Band

E_g

9

8

10

* — excited state
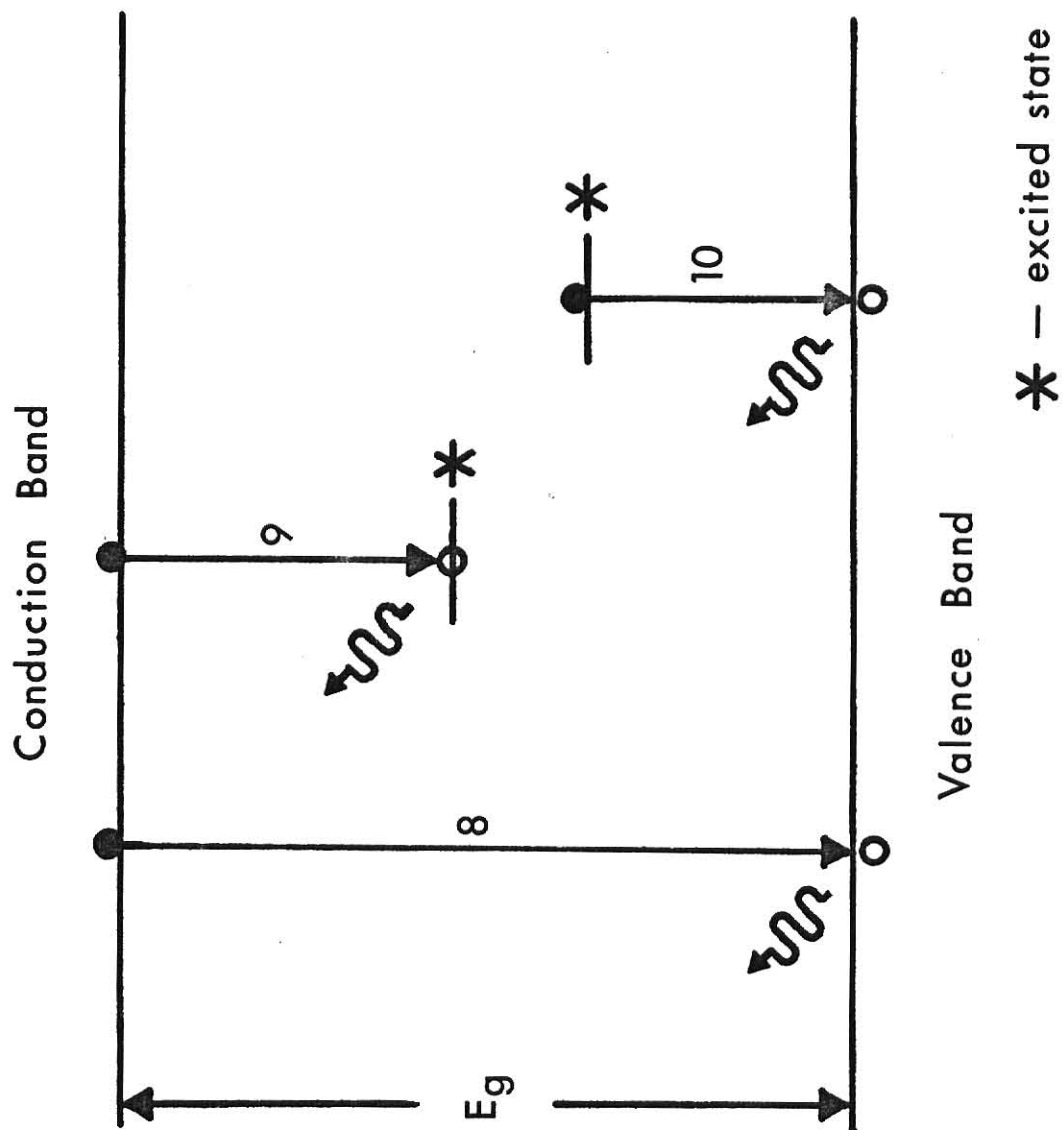
close enough to be thermally promoted into the band. Transition 3 corresponds to absorption, raising an electron from the valence band to an unoccupied imperfection level, producing a free hole and an electron bound in the neighborhood of the imperfection.

Once electrons and holes have been freed by absorption of photons of sufficient energy, they will remain free until they are captured at an imperfectio see Fig. 2. These capturing centers can be classified in two groups:[19,25] 1) trapping centers and 2) recombination centers. In a trapping center, the probability that the captured charge carrier will be thermally freed to the nearest band is large compared to the probability of recombining with a carrier of opposite sign. In a recombination center, the probability for thermal freeing is small compared to that for recombination. Figure 2 shows trapping and thermal release of electrons in electron traps by transitions 5 and 5' and trapping and thermal release of holes in hole traps by electron transition 4 and 4'. The capture of an electron is shown by transition 7 and the capture of a hole by an electron transition 6 in recombination centers.

There are three types of recombination transitions shown in Fig. 3. The free electron may directly combine with a free hole, depicted by transition 8. Transition 9 depicts the capture of a free electron at an excited recombination center containing a hole and transition 10 depicts a free hole being captured at an excited recombination center containing an electron.

The spectral response of the photoconductor will be determined by transitions 1, 2a, 2b, 3. The free carrier lifetime will be determined by transitions 4, 5, 6, 8, 9 and 10. Transitions 4, 5, 6 and 7 frequently determine the speed of response. Optical and thermal quenching of the

10

photoconductivity corresponds to transitions 3 and 4'.

Characteristic Relations of Photoconductivity

The conductivity of a material with free electrons and free holes is given by[9,19,23,25,26]

$$\sigma = ne\,\mu_e + pe\,\mu_h \quad , \tag{1}$$

where σ is the conductivity, e is the charge of the carrier, μ_e and μ_h are the mobilities of the electrons and holes, respectively and n and p are respectively the concentrations of free electrons and free holes. For simplicity in this discussion, Equation 1 will be examined for only one type of free charge carrier. The resulting equation is applicable to either free electrons or free holes. Thus Equation 1 becomes

$$\sigma = ne\,\mu \quad . \tag{2}$$

A change, Δn, in the density of free charge carriers, or a change, $\Delta \mu$, in the mobility of the free carriers, will contribute to a change in the conductivity, $\Delta \sigma$. Using Equation 2, $\Delta \sigma$ is

$$\Delta \sigma = e\mu\Delta n + en\Delta\mu \quad . \tag{3}$$

The first term, $e\mu\Delta n$, represents the conductivity change due to a change in the density of free charge carriers. For steady illumination, the equilibrium number of charge carriers is given by

$$n = g\tau \quad . \tag{4}$$

It can be seen that a change in n requires a change in g, the number of carriers freed/unit volume/unit time, or a change in τ, the mean lifetime of the carrier in the free state. At a specified temperature, g could be changed by either a change in the incident photon flux or the absorption coefficient. It has been observed for the alkali halides that the quantum efficiency for the production of free charge carriers varies slowly with decreasing temperature until a temperature characteristic of the particular alkali halide is reached. Below this temperature the quantum efficiency decreases rapidly.[3,4,7,15,16] Since g is directly proportional to the quantum efficiency, a decrease in temperature would result in a change in the density of free charge carriers.

The other possibility is that the mean lifetime of the free carrier can change. A change in mean lifetime can result when there is a change in the relative importance of the various mechanisms which govern the rates of carrier removal from and emission into the conduction band. For example, as the light intensity is increased trapping levels may become

filled and a corresponding increase in the lifetime of photogenerated carriers may be observed.[19,23,25]

The second term in Equation 3, $en\Delta\mu$, represents the conductivity change due to a change in the mobility of the free carrier. There are several possibilities that result in a mobility change.

1) The formation of space charge in the volume of photoexcitation will reduce the mobility. Space charge can result from; a) Non-uniform illumination throughout the crystal; b) when the electrodes cannot supply or drain off charge carriers freely from the crystal;[19] c) one type of free charge carrier being trapped at defect centers orders of magnitude faster than the opposite type of carrier. This build up of charge will increase the Coulombic barriers that act as scattering centers for the mobile carrier.[24]

2) The presence of charged scattering centers, which during photo-excitation of the carriers have their charge changed by capture of a carrier.[19]

3) Change in crystal temperature will change the mobility.[3,4,15,26,27] At high temperature, scattering by optical phonons limits the mobility. As the temperature decreases the mobility is limited by the crystal purity.[26,27]

Photoconductivity from Defect Centers

The exposure of alkali halides to ionizing radiation promotes electrons from the valence band to the conduction band and they can be trapped at halogen-ion vacancies. This defect center resembles a hydrogen atom and is called an F center.[5,7,8,12] Under prolonged irradiation, other defect centers, aggregates of the F center, are formed. Two F centers as nearest

13

neighbors constitute an M-center, three adjacent F centers an R center and so on.[3,4,8,10,12,20,25] There are also defect centers formed by impurity atoms or ions in the crystal. When the impurity is positive and divalent, the defect centers are known as Z centers.[3,4,8,12]

All these defect centers have localized energy levels in the forbidden energy gap of the crystal. The transition of the electron from the ground state to an excited state upon the absorption of a photon gives rise to an absorption band characteristic of the defect center. Since the F center resembles a hydrogen atom, higher excited states of the F center would be expected.[4,7] These higher states have been observed in several of the alkali halides and are known as K and L bands.[3,4,7,8]

It is experimentally observed that the peak position of the optical absorption band shifts to higher energy and the full width at half maximum, FWHM, decreases with decreasing temperature.[3,4,8,31] Using the simplest model for the F center, in which the trapped electron will be treated as a particle in a box, it is possible to qualitatively explain the behavior of the F center optical absorption band with a change in temperature.[31,32,33] The energy between the ground state and the first excited state for a particle in a box is

$$E_2 - E_1 = \frac{3\pi^2 \hbar^2}{8ma^2} \quad , \tag{5}$$

where m is the mass of a free electron, $\hbar$ is Planck's constant divided by 2π and "a" is the nearest neighbor distance.[31,32] For LiF at 293°K, "a" is 2.013 Å.[34] The energy, calculated from Equation 5, is 6.9 eV. This compares to an experimentally observed value of 5.0 eV. At 73°K, "a" is

14

2.003 $\overset{\circ}{A}$[34] and the peak position of the absorption band has shifted to 6.97

eV. Experimentally the observed shift is to 5.12 eV. Qualitatively it can

be seen that the shift can be explained by the thermal contraction of the

lattice.[31,32,33] The width of the band arises from the interaction of the

F center with the vibration of the neighboring ions about their zero-point

position.[31,32,33] As the temperature decreases, the average amplitude of

the thermal vibrations of the ions will decrease.

Using the particle-in-a-box model, the decrease of the average ampli-

tude of the thermal vibrations will result in a decrease in the variation

of the dimensions of the box. Qualitatively it is seen that a decrease in

the variation of the dimensions of the box will result in the narrowing

of the width of the absorption band.[31,32,33]

The particle-in-a-box model of an F center is the simplest model used

for calculating the energy levels of the F center. More exact calculations

attempt to use various approximations and potential energy terms that take

into account such contributions to the energy levels as electronic polarization,

the dielectric constant, the effective mass of the electron in the F center

and the temperature dependence of the F center absorption band. A very

good discussion of these calculations is found in Fowler[8] and Schulman and

Compton.[4]

Photoconductivity would be observed from F center, M centers, R centers,

and Z centers for transitions 2a and 2b in Fig. 1. In the alkali halides,

transitions of type 2b are the ones of most interest and they have been

observed for all the defects mentioned previously.[4,8,13,14,15,16,17,18]

If there is to be photoconductivity from a 2b transition, the energy

difference between the excited state and the conduction band minimum must

be small, on the order of a few tenths of an electron volt,[8,19] so the

15

electron can be thermally freed from the excited state. Thus studying the photoconductivity as a function of temperature would lend itself to the determination of the thermal ionization energy of the defect producing the photoconductivity.[3,4,8,9,20,23,25]

For the specific case of F centers in LiF, it has been determined that the width of the forbidden energy gap is approximately 13.4 eV[28] and the ground state of the F center is 5.04 eV above the top of the valence band.[29] At room temperature, the first excited state of the F center is 5.0 eV above the ground state.[3,4] This would mean the first excited state of the F center is approximately 3.5 eV below the conduction band minimum and photoconductivity from the first excited state of the F center in LiF would not be possible for a single photon absorption process. Thus photoconductivity observed in LiF for low incident photon fluxes over the energy range investigated must be generated from some other defect.

III.   EXPERIMENTAL PROCEDURE

Optical absorption spectra and photoconductivity excitation spectra of gamma-irradiated LiF were observed in the spectral range of 700 nm to 200 nm and 370 nm to 200 nm, respectively. The optical absorption and photoconductivity spectra were measured with unpolarized light and light polarized in the [011] and [0$\bar{1}$1] directions relative to the crystal axes. In all experiments the wave vector of incident light was in the [100] direction through the crystal lattice.

Experimental Samples

The LiF crystals were purchased from Harshaw Chemical Corporation in 1972. Harshaw stated that the possible impurities present in the samples were Aℓ, Ca, Fe, and Mg, with concentrations of 1-3 ppm. To determine what impurities were present, a qualitative Neutron Activation Analysis was run on two crystals. The impurities Aℓ, Na and Cℓ were found. The specifics of the Neutron Activation Analysis are given in Appendix I.

The sample crystals were cleaved from larger single crystals of LiF. The dimensions of the samples used for the optical absorption measurements were 1.0×1.0×0.5 cm. The photoconductivity measurements were made with 0.5×0.5×0.1 cm samples.

Thermal Annealing

Prior to gamma irradiation, all samples were annealed for 24 hours at 450°C. They were then quick quenched to room temperature, in air, by

17

placing the Pyrex beaker containing the samples on a large piece of stainless steel. The purpose of the quick quenching was to freeze in the uniform distribution of vacancies produced during the high temperature anneal.

After the sample was gamma-irradiated, it was annealed at 100°C for 30 minutes and again quick-quenched to room temperature. The purpose of this anneal is to destroy the larger F-center aggregates so as to eliminate any possible interactions between these centers and the centers of interest. The quick quenching's purpose was to freeze in those defects left after the 100°C anneal.

Gamma Irradiation

The irradiation of the samples was carried out in the irradiation chamber of the Gamma cell (AECL 220) located in the Nuclear Engineering Department. The Gamma cell was loaded on March 15, 1964 with 3,963 curies of Cobalt-60.

To irradiate a sample, a polyethylene disk was placed in the irradiation chamber of the Gamma cell.[30] The purpose of the disk was to position the samples in the irradiation chamber so that they would receive the same dose as a sample that had been positioned in the geometric center of the chamber. Thus it would be possible to irradiate several samples at the same time, at the same dose rate. The position is located at 2-3/4 inches above the base of the chamber and two inches from the center axis of the chamber.[30] The dose rate at this position was 24.2 rads per second, as of February 1, 1975. The sample was placed on the disk and the door to the irradiation chamber closed. A timer located on the operator's panel was then set for the desired exposure time and the irradiation chamber was

lowered into the cell. After the sample had received the required dose,
the timer activated a travel mechanism which raised the chamber back out
of the cell. The above procedure was reversed and the sample removed
from the irradiation chamber.

Optical Absorption and Bleaching Measurements

A Cary-14 Spectrophotometer was used to measure the optical absorption
spectra. The optical absorption spectra were measured with unpolarized
light and plane-polarized light with the polarization in either the [011]
or the [01̄1] direction. For all the measurements the k vector of the
light was in the [100] direction relative to the crystal axes. Figure
4 gives the orientation of the polarization vectors and the k vector
of the incident light relative to the crystal axes.

The self-absorbance spectrum of the unirradiated sample was measured
first and used as the background spectrum for that sample. This background
spectrum was subtracted from the spectrum of the irradiated sample to show
the effect of the gamma irradiation.

The optical absorption spectra were observed at temperatures of 300°K
and 90°K. A schematic of the dewar is shown in Fig. 5. The sample was
held on the copper cold finger by Eccotherm TC-4 conducting grease, made
by Emmerson and Cummings Inc., Canton, Massachusetts.

Figure 6 shows the experimental arrangement for optically
bleaching the samples. The samples were bleached with either unpolarized
light or light polarized in the [011] direction. The wavelength of the
bleaching light was 254 nm at 300°K and 244 nm at 90°K. A Bausch and
Lomb, Model HP-100, 100 watt Mercury Arc Lamp and Power Supply, coupled
with a Jarrell-Ash, Model 82-410, 0.25 meter Ebert Monochromator, was used

19

FIGURE 4

Crystallographic representation of the direction of propagation
and the direction of the polarization of the incident light.
Dark arrows denote the polarization of the incident light
relative to the crystal axes. The k vector of the incident
light was in the [100] direction.

$[001]$

$[010]$

(100)
cube
face

$[011]$

$[0\bar{1}1]$

$[100]$
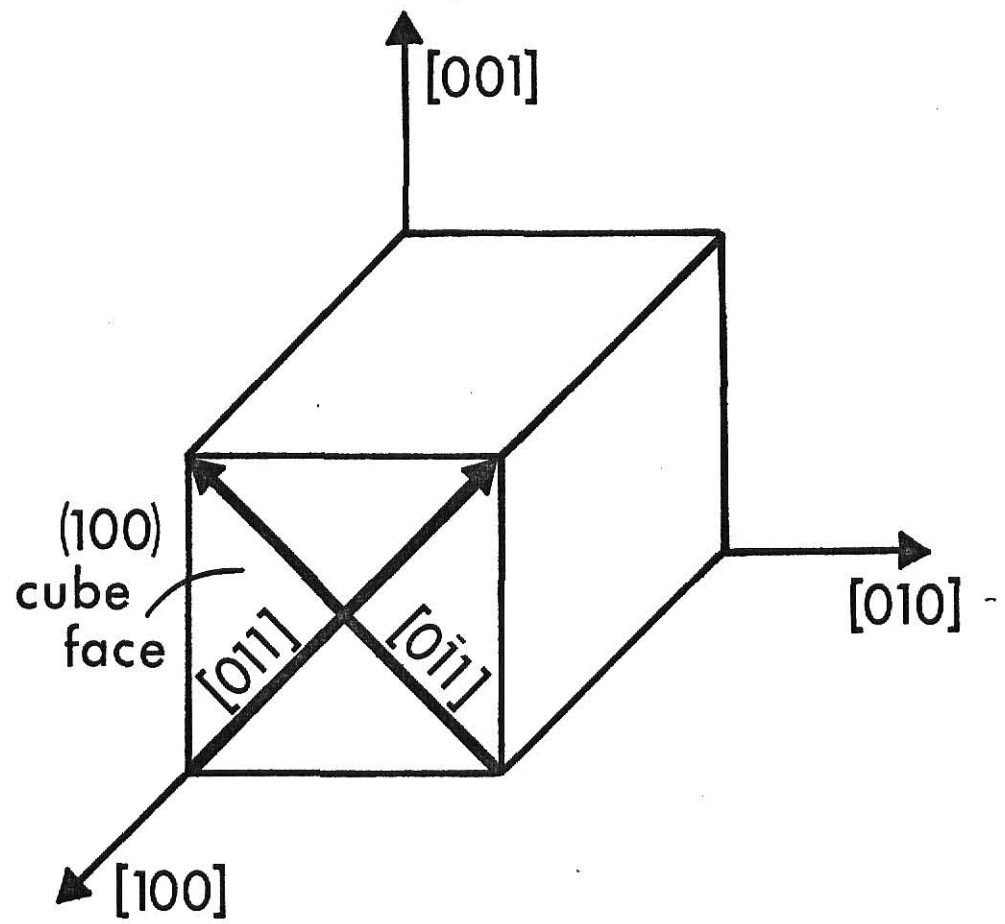
FIGURE 5

Glass dewar and sample holder for optical absorption measurements.

$\overline{\$}^{12}/_{30}$
Joint

to Vacuum
Line

¼" Plywood

Liquid
Nitrogen

Pyrex
Glass

$\overline{\$}^{29}/_{42}$
Joint

Kovar Seal

Copper Cold
Finger

LiF Sample

Incident
Light

UV
Polarizer

Quartz
Windows

23
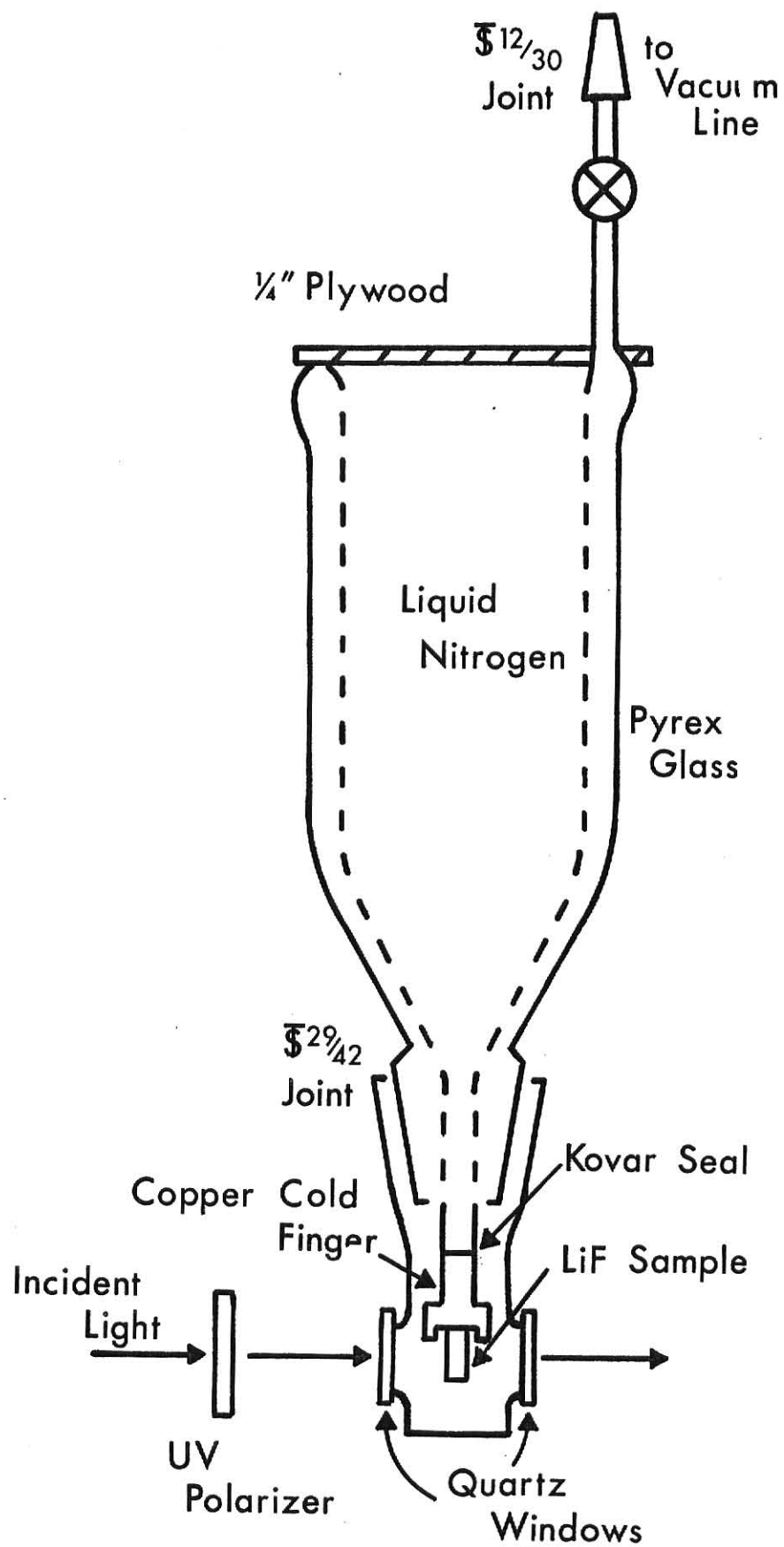
FIGURE 6

Experimental arrangement used in determining the effect of

optical bleaching on the optical-absorption spectra.

B&L 100 Watt
Mercury Lamp

Jarrell–Ash

Monochromator

2.4 cm

Shutter

7.3 cm

UV Polarizer

2.7 cm

Quartz Window

2.0 cm

LiF Sample

Quartz Window
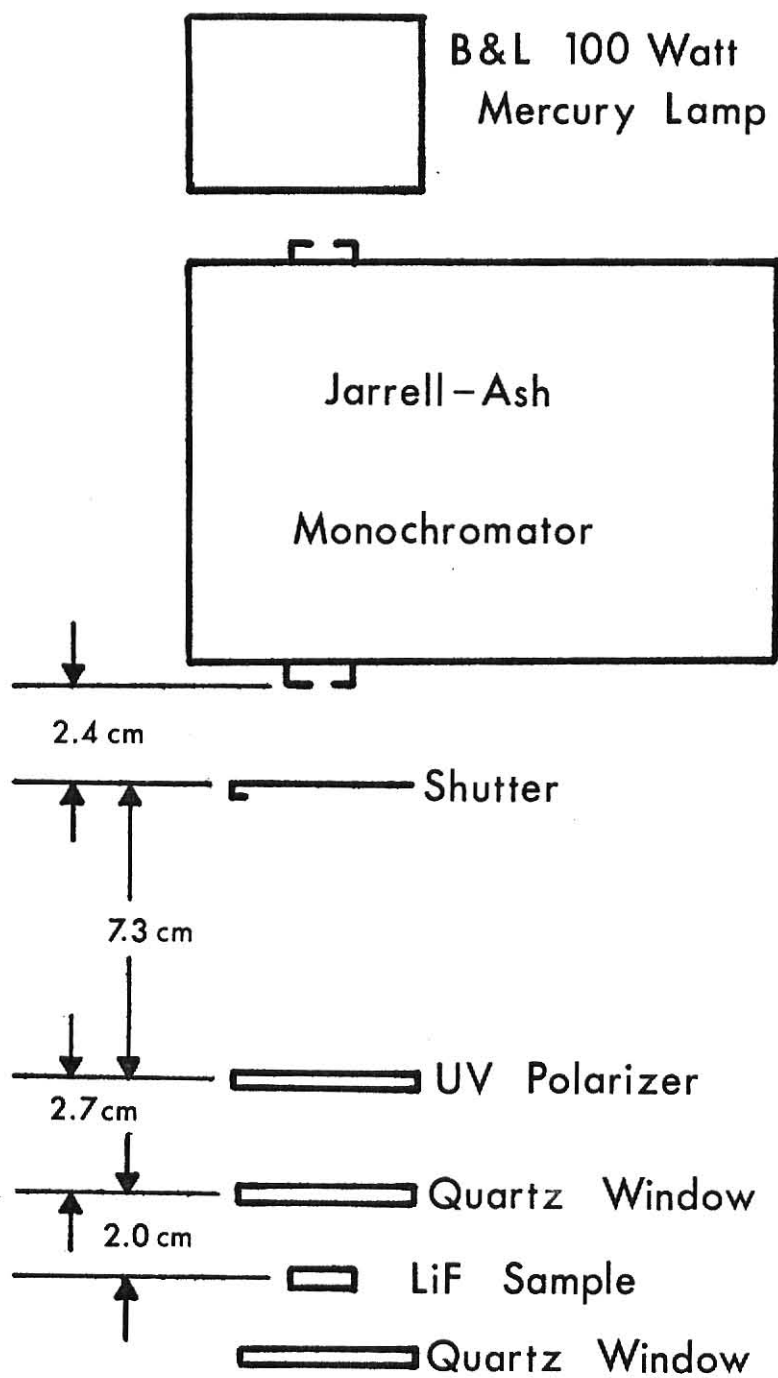
as the bleaching source. The Jarrell-Ash monochromator has a dispersion of 1.6 nm/mm in the ultraviolet. A one millimeter exit slit was used giving a bandpass of 1.6 nm. A linear polarizer made by Polacoat Inc. was employed to polarize the light from the monochromator when bleaching with [011] polarized light. The spectral range of the polarizer was 240 nm to 400 nm.

Photoconductivity Measurements

Figures 7, 8 and 9 show the experimental equipment that was used for the photoconductivity measurements. The light source was composed of a LPS 251 Lamp Power Supply, LH 150 Lamp Housing and 150 watt Xenon Lamp, made by Schoeffel Instrument Corporation. The LH 150 Lamp Housing was provided with a focusing lens and a shutter. This light source, coupled with a Bausch and Lomb 33-88-01 Grating Monochromator, was used for photoexcitation and bleaching of the samples. The Bausch and Lomb monochromator had a 5 nm bandpass determined by a combination of a 2.68 mm entrance slit, 1.50 mm exit slit and a 3.2 nm/mm dispersion in the ultraviolet.

The sample was placed in a vacuum chamber that mounted on the monochromator. A quartz window allowed the light from the monochromator to enter the vacuum chamber and strike the surface of the sample. The sample holder was mounted on a liquid-nitrogen cold finger in the vacuum chamber, see Fig. 9. Between the cold finger and the sample holder a thin layer of Eccotherm TC-4 conducting grease was applied to give good thermal contact. With this arrangement it was possible to vary the sample temperature from 85°K to 300°K. The temperature of the sample was measured with a copper-constantan thermocouple attached close to the sample on the

FIGURE 7

Block diagram of the experimental equipment used for the photoconductivity measurements

```
┌─────────────────┐   ┌─────────────────┐   ┌─────────────────┐
│    LPS 251      │   │     LH150       │   │    LP410 FM     │
│                 │   │                 │   │                 │
│   Lamp  Power   ├───┤  & 150 Watt     │   │   Regulated     │
│                 │   │                 │   │                 │
│     Supply      │   │    Xe Lamp      │   │  Power Supply   │
└─────────────────┘   └────────┤────────┘   └─────────────────┘
                               ▒▒                    │
                               ▒▒                    │
                      ┌────────┤────────┐   ┌─────────────────┐
                      │ B&L   33-88-01  │   │    H-P Mosely   │
                      │                 ├───┤                 │
                      │    Grating      │   │   7004A-116     │
                      │                 ├───┤                 │
                      │  Monochromator  │   │    Recorder     │
                      └────────┤────────┘   └────────┤────────┘
                               ▒▒                    │
┌─────────────────┐   ┌────────┤────────┐   ┌────────┤────────┐
│   H-P  6110A    │   │    Vacuum       │   │    Cary  401    │
│                 │   │    Chamber      │   │                 │
│   D.C.  Power   │   │      &          │   │   Electrometer  │
│                 │   │    Sample       │   │                 │
│     Supply      │   │    Holder       │   │    & Preamp     │
└────────┬────────┘   └───┬────┬────────┘   └───┬─────────────┘
         │                │    │                │
         └────────────────┘    │    ┌───────────┘
                        ┌───────┤────┤────┐   ┌─────────────┐
                        │  L&N  7554,     │   │             │
                        │                 │   │     Ice     │
                        │  Type K-4,      │   │             │
                        │                 │   │    Bath     │
                        │  Potentiometer  │   └─────────────┘
                        └────────┤────────┘
                        ┌────────┤────────┐
                        │  Keithley  155  │
                        │                 │
                        │      Null       │
                        │                 │
                        │    Detector     │
                        └─────────────────┘
```

28
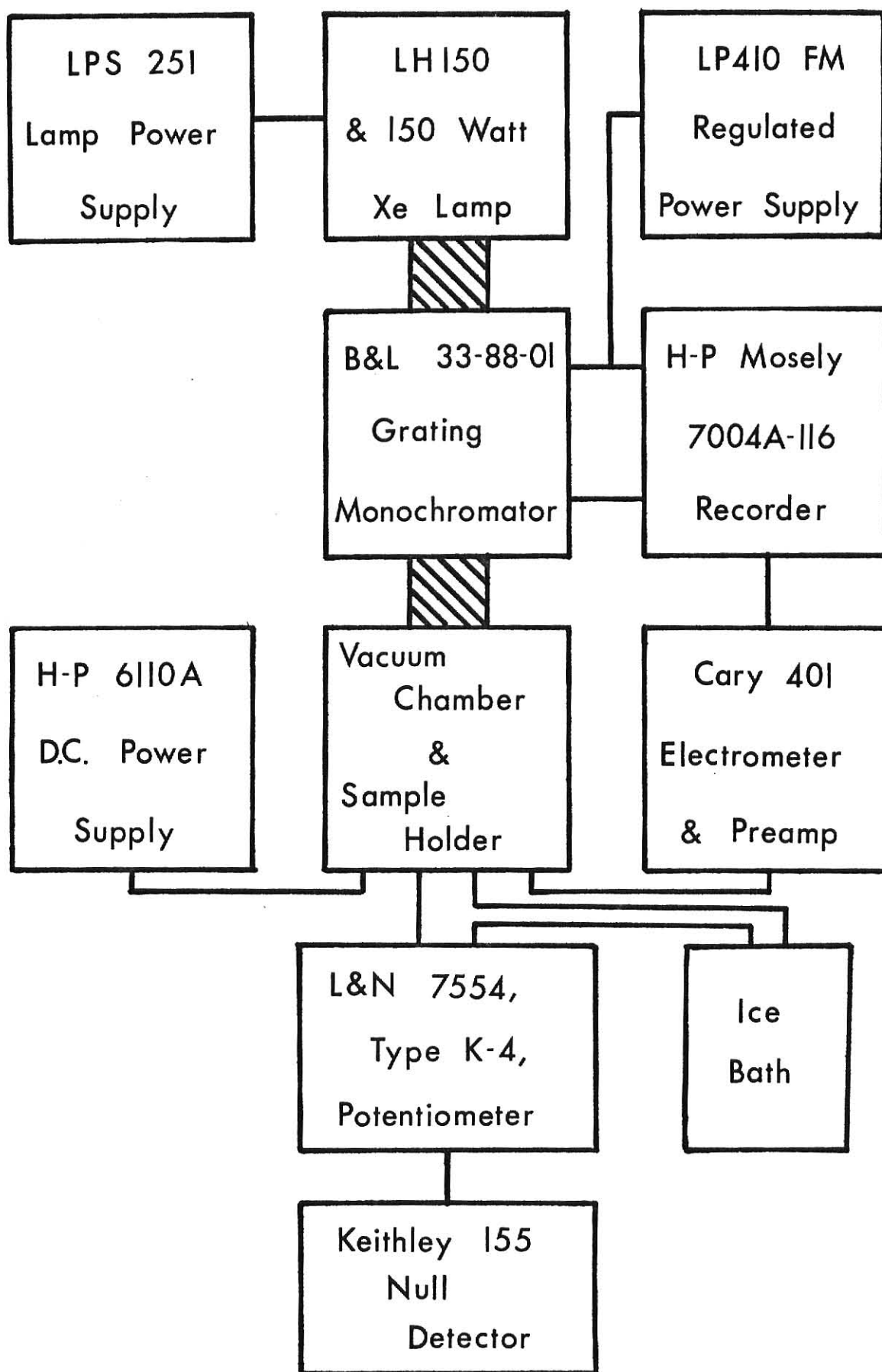
FIGURE 8

Top view of the Bausch and Lomb monochromator and vacuum

chamber used in the photoconductivity measurements

Xe Lamp

Focusing Lens

Shutter

2.68mm Entrance Slit

B-L 33-88-01 Grating Monochromator

±V from LP410 FM

$+V_1$

$-V_1$

$-V_2$

$+V_1$ to

H-P 7004A-116

10K ohm Pot.

1.5mm Exit Slit

9cm

Quartz Window

Nickel Screen

Biasing Electrode

LiF Sample

Copper Cold-Finger

to Cary 401

Thermocouple

Bias from H-P 6110A

Vacuum Chamber

to Vacuum System

FIGURE 9

Side view of the vacuum chamber, cold finger and sample holder used in the photoconductivity measurements.

Stainless Steel

Endotherm TC-4

to Vacuum System

Foam Rubber

Liquid Nitrogen

Guarded Electrode

Cu Cold-Finger

Sample Holder

LiF Sample

Quartz Window

32

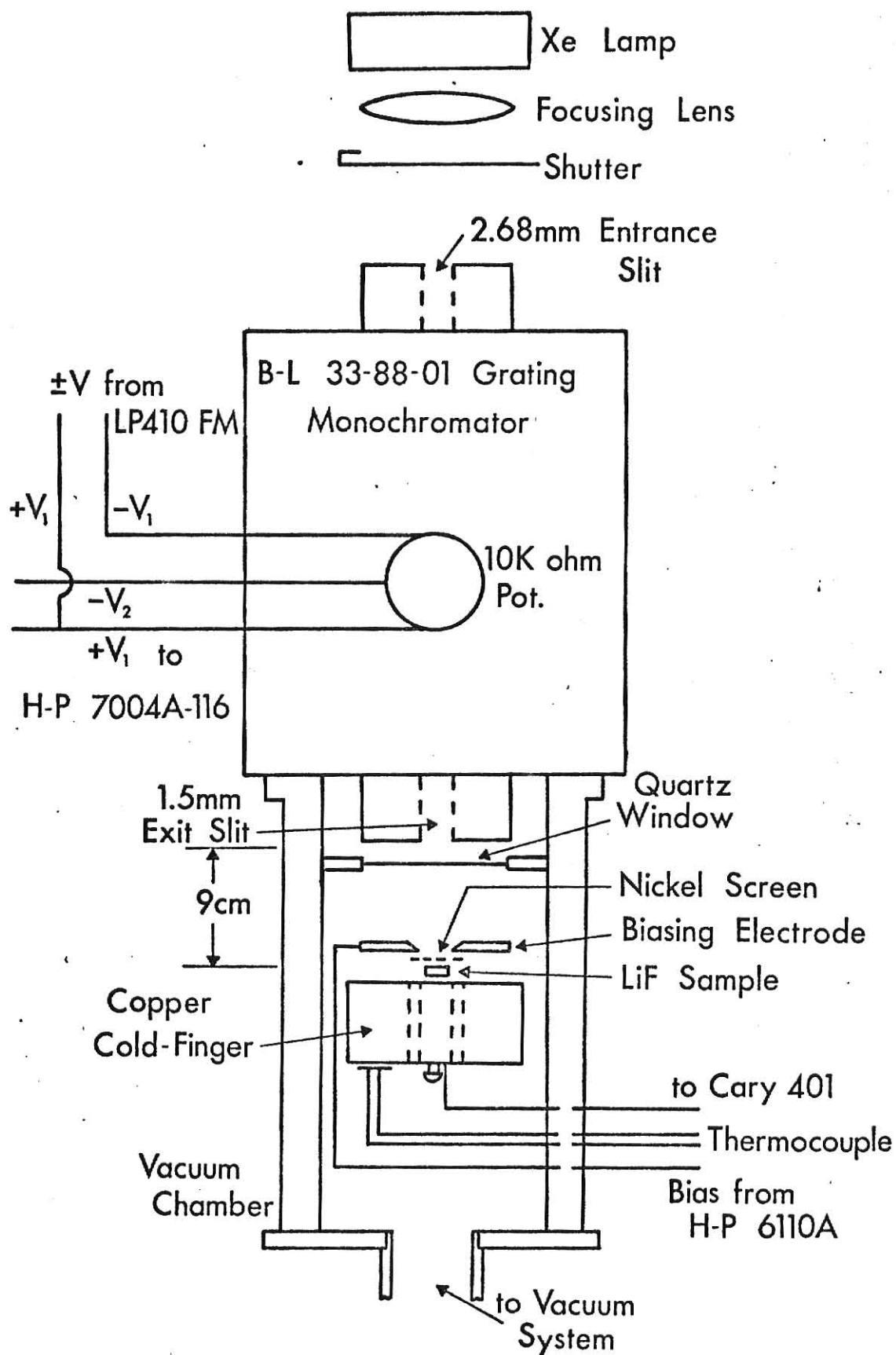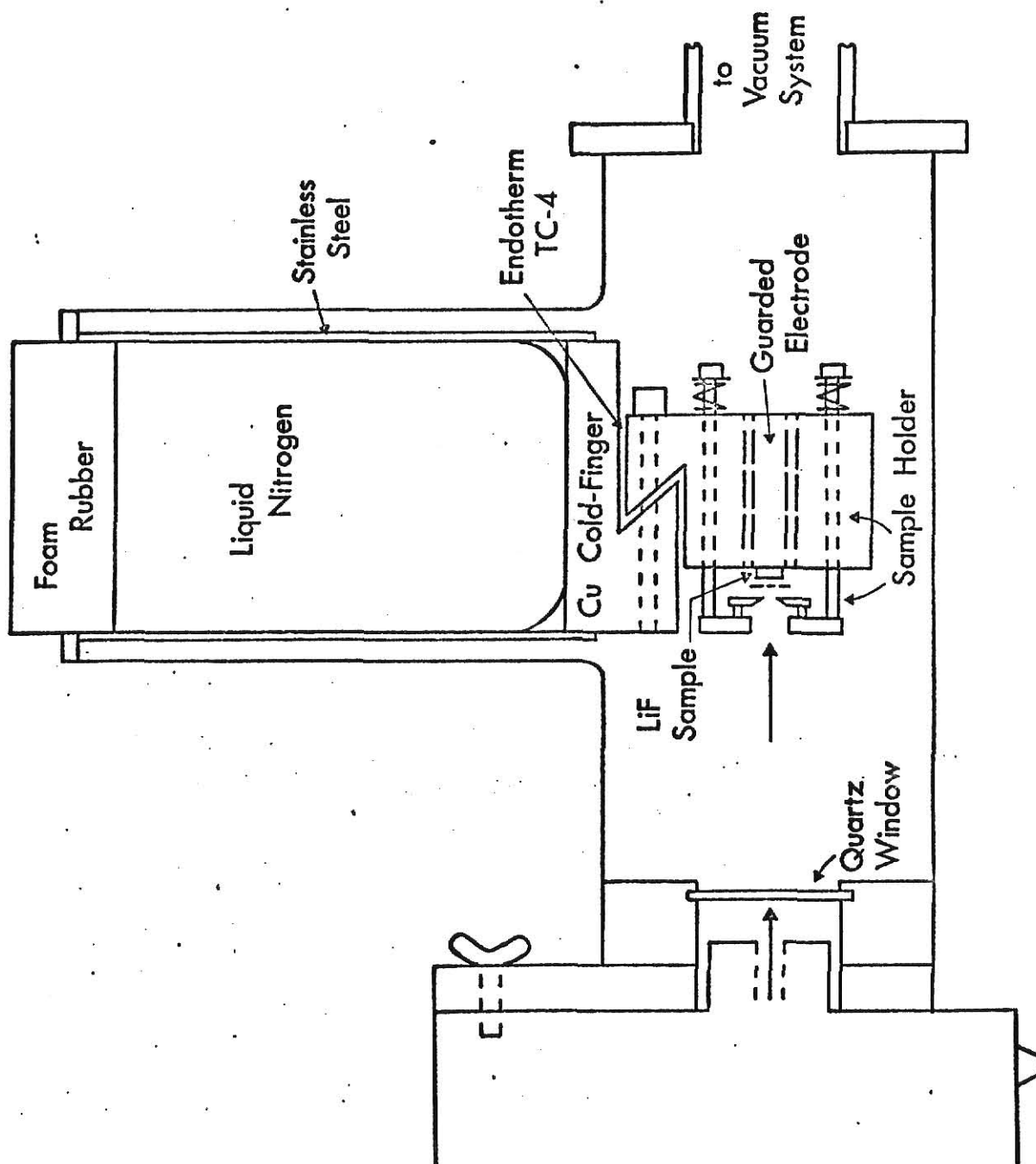sample holder and held in place with General Electric Adhesive Varnish, no. 7031. The reference junction of the thermocouple was held at 0°C in an ice bath and the thermocouple's e.m.f. was measured with a Leeds and Northrup, Model 7554, Type K-4, Potentiometer and a Keithley, Model 155, Null-Detector Microvoltmeter.

The front sample electrode, hereafter referred to as the biasing electrode, was biased using a Hewlett-Packard 6110A D.C. Power Supply. Positive or negative voltages up to 3000.0 volts were obtainable from this power supply. The biasing electrode had a 0.126 cm^2 hole to illuminate the sample. To ensure that the applied electric field was fairly uniform across the sample, a nickel screen of mesh size 70 squares per inch was placed between the sample and the biasing electrode. The absorbance of the nickel screen was 0.05 absorbance units.

A Cary 401 Vibrating Reed Electrometer was used to measure the change in conductivity of the sample due to photoexcitation. The actual parameter the electrometer measured was the change in the voltage drop across the electrometer input resistor. Since the voltage drops measured were small, it was necessary to electrically guard the input to the electrometer against leakage currents. This was accomplished by placing a guard ring around the rear sample electrode, the input to the electrometer, and operating the electrometer in the current mode. When operated in this mode, the electrometer reduces, by a feedback circuit, the voltage change at the input terminal with respect to ground by a factor of 0.001. The output from the electrometer was recorded on the Y-axis of a Hewlett-Packard 7004A-116 X-Y Plotter. The incident photon wavelength was recorded on the X-axis of the plotter. Since the output signal of the electrometer is dependent on the incident photon's wavelength, a photoconductivity spectrum

33

of a sample can be plotted by scanning over a range of photon wavelengths.

For this purpose a wavelength drive was constructed and connected to the wavelength control of the monochromator. The wavelength drive consisted of an A.C. synchronous motor and gear reduction, a 10,000 ohm, 3/4 turn potentiometer and a Lambda Regulated Power Supply, Model LP410 FM. The potentiometer acted as a voltage divider as shown in Fig. 8. As the motor turned the wavelength control, it also turned the potentiometer, thus sending a voltage to the plotter that was proportional to the wavelength. The linearity of the potentiometer determined the calibration of the X-axis. The wavelength scanning rate was determined by the motor and the gear reduction. The scanning rate used was 2.2 nm/sec.

The photoconductivity samples were bleached with unpolarized light or light polarized in the [011] direction. The same experimental arrangement employed for the photoconductivity measurements was used for bleaching the samples with unpolarized light, see Figs. 8 and 9. When light polarized in the [011] direction was needed, the polarizer was placed between the quartz window and the exit slit of the Bausch and Lomb Mono-chromator.

Determination of the Photon Flux of the Xenon and Mercury Lamps

The photon fluxes of the Xenon and Mercury Lamps were determined by use of a Laser Power Meter, Model 3600, made by Scientech Inc. An asbestos cover was fabricated to minimize the response produced from extraneous light sources. The Power Meter's output was measured using a Keithley, Model 155, Null-Detector Microvoltmeter. The output calibration for the Power Meter was 1 millivolt equals 10 milliwatts. Further details are

given in Appendix II.

given in Appendix II.

IV.   RESULTS AND DISCUSSION

Optical absorption spectra and photoconductivity excitation spectra
of LiF were measured with unpolarized light and plane-polarized light,
with the polarization vector in the [011] and [0Ī1] directions relative
to the crystal axes.   The optical absorption spectra were measured in
the spectral range from 700 nm to 200 nm at temperatures of 90°K and
300°K.   The photoconductivity excitation spectra were measured in the
spectral range from 370 nm to 200 nm at temperatures from 85°K to 300°K.

The effect of optical bleaching, with light corresponding to the F center
absorption band maximum, was observed by studying changes in the optical
absorption spectra and the photoconductivity excitation spectra.   In
the optical absorption bleaching measurements, the bleaching light was
either [011] polarized light at 244 nm at 90°K or unpolarized light at
254 nm at 300°K.   In the photoconductivity bleaching measurements, the
bleaching light was either unpolarized light or light polarized in the
[011] direction at 254 nm at 300°K.

Optical Absorption of Irradiated LiF

Figures 10, 11 and 12 show the optical absorption of LiF versus
photon energy after exposure to 0.12 Mrad of gamma radiation.   Figure
10a shows the optical absorption spectrum of LiF at 300°K and Fig.
10b the optical absorption spectrum of LiF at 90°K.   Both are measured
with unpolarized light.   Figure 10a consists of the prominent F center

36

FIGURE 10

Optical absorption spectra of irradiated LiF measured with unpolarized light at 90°K and 300°K. Curve (a) is the optical absorption measured at 300°K. Curve (b) is the optical absorption measured at 90°K. Absorbed Dose - 0.12 Mrad.
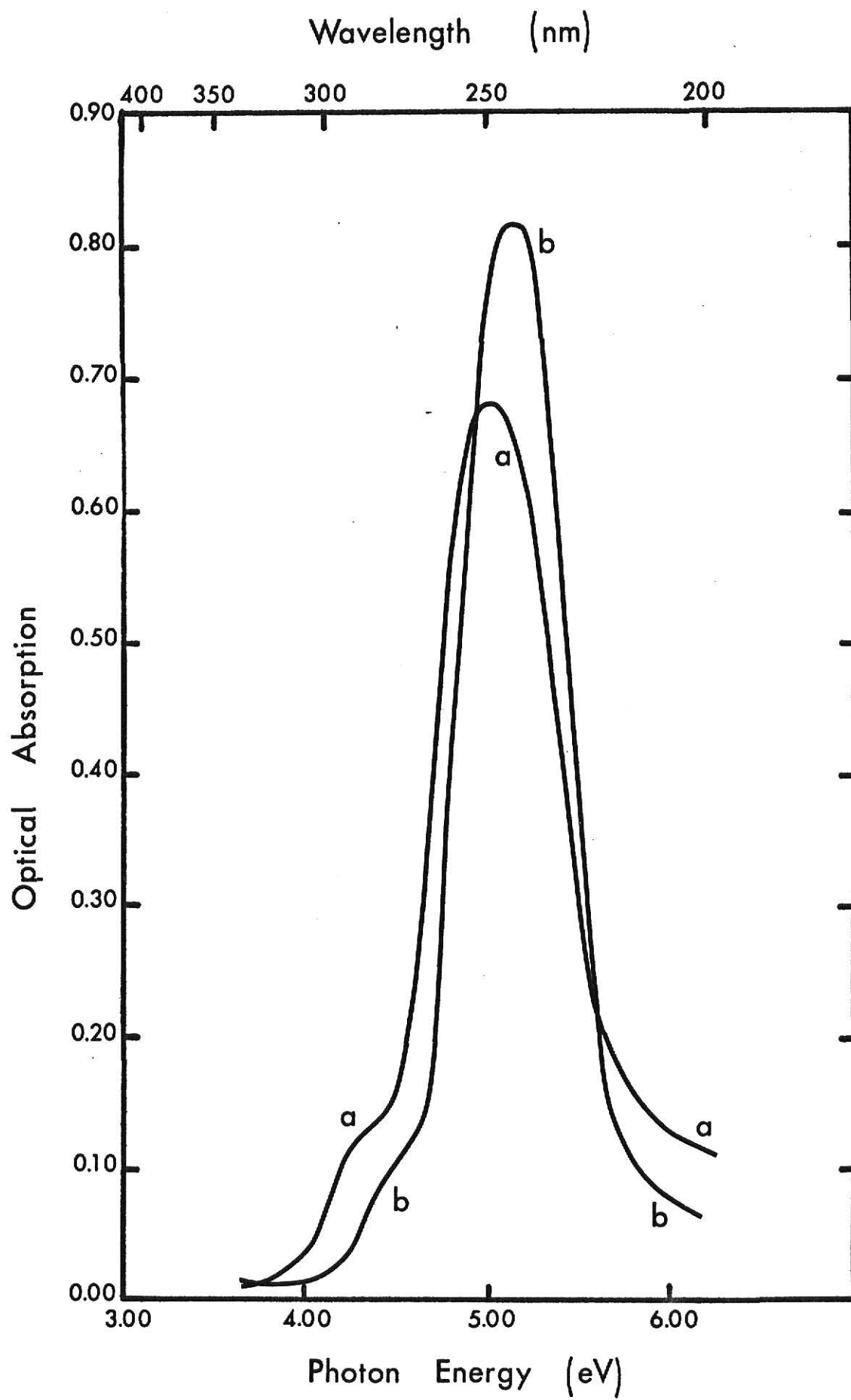
absorption band at 5.0 eV and a small unresolved absorption band, hereafter referred to as the Y center absorption band, on the low-energy side of the F center around 4.4 eV. When Figs. 10a and 10b are compared, it is observed that the peak position of the F center absorption band has shifted to 5.1 eV and the peak position of the Y center absorption band has shifted to ∿4.5 eV. It is also observed that the full width at half maximum (FWHM) of the F center absorption band has decreased from 0.81 eV at 300°K to 0.67 eV at 90°K.

The shift of the peak position of the F center absorption band, to a higher energy with decreasing temperature, can qualitatively be understood by the particle-in-a-box model of the F center. From Eq. 5 it is seen that the difference in energy between the ground state and the first excited state of the particle in a box is inversely proportional to the square of the size of the box. For this model of the F center, the particle is the electron and the box is the negative ion vacancy. When the lattice is cooled, thermal contraction will decrease the size of the box. The reduction of the size of the box will result in increasing the difference between energy levels. As a consequence the peak position of the absorption band will shift to higher energy.

The narrowing of the FWHM of the F center absorption band can also be qualitatively explained by the particle-in-a-box model of the F center. The FWHM of the absorption band is a result of thermal vibrations of the Li^{+1} ions, surrounding the negative ion vacancy, about their zero point position. The amplitude of the vibration will give a range of possible values for the size of the box. As the temperature is decreased,

39

the decrease in the amplitude of the thermal vibration will result in a smaller range of possible values for the size of the box. Thus the FWHM of the absorption band will decrease with decreasing temperature, until the amplitude of the thermal vibrations has reached its minimum value. After this value is reached, the FWHM of the absorption band will not decrease if the temperature is further lowered.

The area under the F center absorption band is proportional to the concentration of F centers, if it is assumed they are sufficiently dispersed so that they do not interact with one another. The concentration of F centers can be calculated using Smakula'a Equation,[4]

$$Nf = \frac{n}{(n^2 + 2)^2} \alpha W(0.87 \times 10^{17}) \quad , \qquad (6)$$

where N is the number of absorbing centers per cm^3, α is the absorption coefficient in cm^{-1} at the peak of the absorption band, W is the FWHM in eV, f is the oscillator strength of the absorbing center and n is the index of refraction at the maximum of the absorption band. The concentration of F centers at 90°K and 300°K should be equal since the F center is thermally stable over the temperature range shown.[3,4,8,10] The calculated concentration of F centers at 300°K is 8.65×10^{15} cm^{-3} and at 90°K is 8.63×10^{15} cm^{-3}.

Figures 11a and 11b are respectively the optical absorption spectrum measured with [011] polarized light and [0$\bar{1}$1] polarized light at 300°K. As in Fig. 10, the optical absorption spectrum consists of the prominent F center absorption band at 5.0 eV and of the Y center absorption band around 4.4 eV. It is observed that the optical absorption of the Y center

FIGURE 11

Optical absorption spectra of irradiated LiF measured with [011]
and [0Ī1] polarized light at 300°K. Curve (a) is the optical
absorption spectrum measured with [011] polarized light, curve
(b) is the optical absorption spectrum measured with [0Ī1]
polarized light. Absorbed Dose - 0.12 Mrad

42
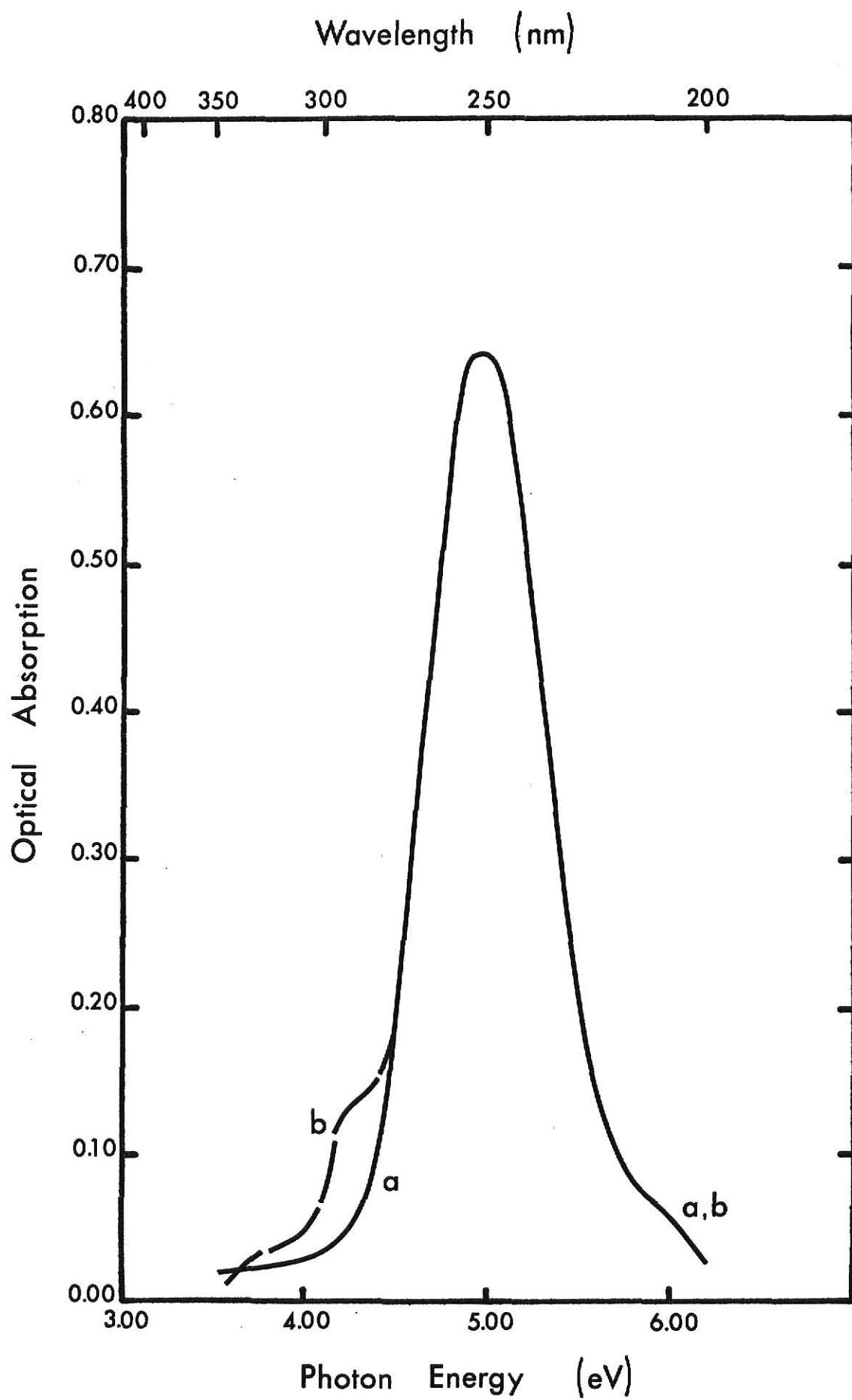
exhibits dichroic behavior for the two polarizations with the optical absorption being larger for the [0$\bar{1}$1] polarized light. Figure 12 shows the dichroic optical absorption of the Y center at 90°K. Figure 12a is the absorption spectrum measured with [011] polarized light and Fig. 12b is the absorption spectrum measured with [0$\bar{1}$1] polarized light.

The dichroism indicates that the number of Y centers oriented in the [0$\bar{1}$1] direction is larger than the number oriented in the [011] direction. There are two possible explanations for the observed dichroism;

(1) The dichroism is present before the experiment is performed;

(2) The dichroism is induced by the experiment.

The first alternative suggests that the manner of crystal growth can induce a preferential orientation of the defect. It is known that the Harshaw Chemical Corporation irradiates the LiF crystals with Cobalt-60 gamma rays to facilitate the cleaving process.[36] Since the manner of crystal growth and the exact cleaving process is not known, this alternative cannot be excluded.

The other alternative is that the dichroism is induced by the experiment. All the samples are annealed at 450°C for 24 hours and quick-quenched to room temperature. This quenching can introduce thermal strains by nonuniform cooling of the sample. It is difficult to imagine how the quenching can induce a strain so that there is the same preferred orientation of the defect in every sample. The samples are irradiated with Cobalt-60 gamma rays and it is difficult to say whether the radiation induced the dichroism because the direction of the gamma rays relative to the crystal axes is not known. The samples are then annealed at 100°C

43

FIGURE 12

Optical absorption spectra of irradiated LiF measured with [011]

and [0$\bar{1}$1] polarized light at 90°K. Curve (a) is the optical

absorption spectrum measured with [011] polarized light. Curve

(b) is the optical absorption spectrum measured with [0$\bar{1}$1]

polarized light. Absorbed Dose – 0.12 Mrad
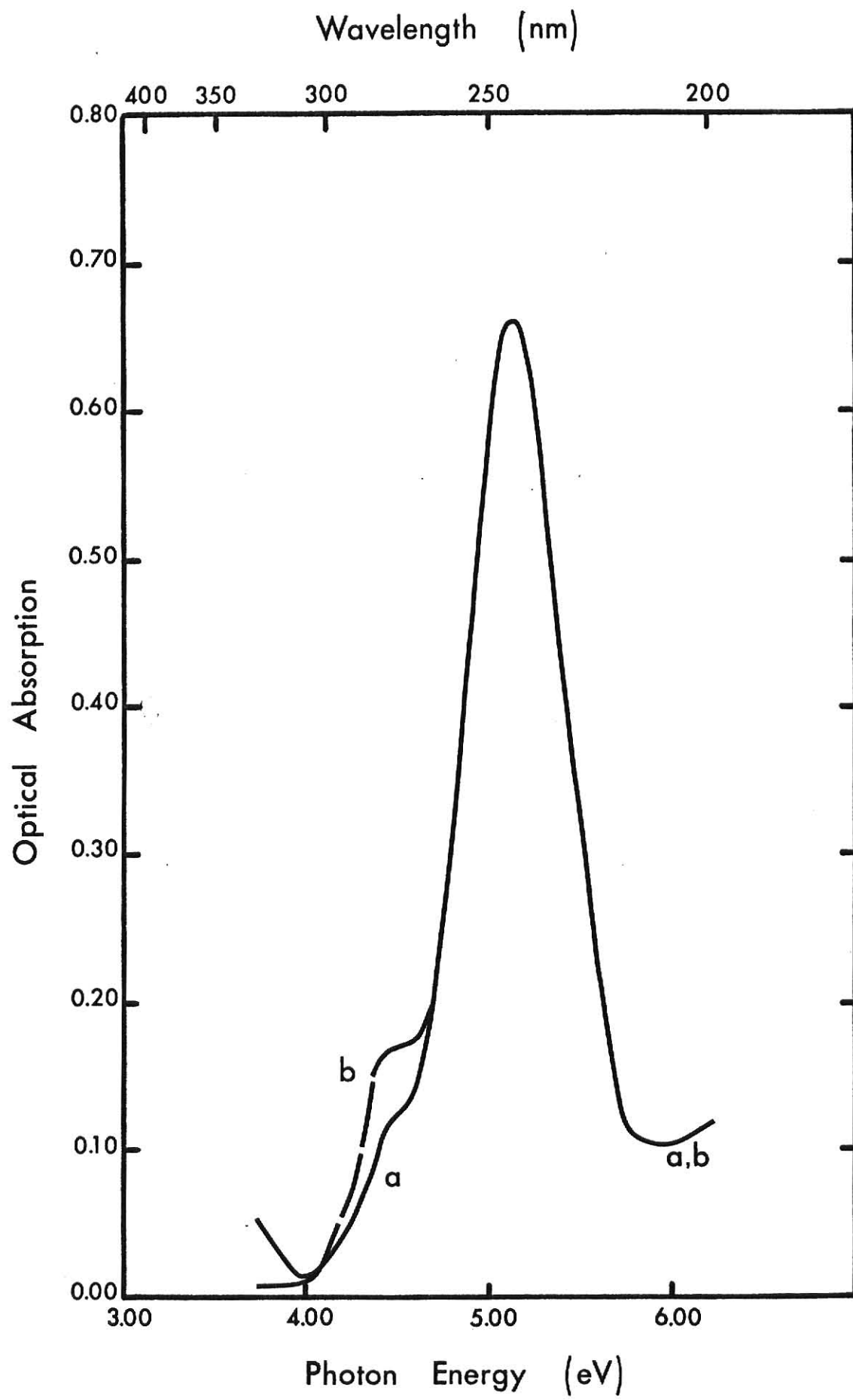
for 30 minutes and quick-quenched to room temperature. This annealing process and this quick quenching do not explain the dichroism.

The optical absorption spectra are always measured in the following order; unpolarized light, [011] polarized light and [0$\bar{1}$1] polarized light. Since there are examples of defects orienting in a preferred direction under the influence of polarized light,[38,39] the optical absorption spectra are measured so that the order is changed to unpolarized light, [0$\bar{1}$1] polarized light and [011] polarized light. No difference is observed in the optical absorption spectra on changing the order in which the measurements are made. This suggests that the defect producing the Y center absorption band prefers an orientation along the [0$\bar{1}$1] direction over the [011] direction. If this is the case, rotation of the sample by 90° about the [100] direction in the crystal would translate the [0$\bar{1}$1] direction into the [011] direction. When the rotation is performed, the dichroism did switch to show the [011] optical absorption larger than the [0$\bar{1}$1] optical absorption.[37] It is concluded that the manner in which the experiment is performed does not induce the observed dichroism.

At this time there is no satisfactory explanation as to why the defect producing the Y center absorption band prefers the [0$\bar{1}$1] orientation over the [011] orientation.

Effect of Optical Bleaching on the Optical Absorption Spectra

The effect of optical bleaching with unpolarized light at 300°K and [011] polarized light at 90°K is observed by the changes in the optical absorption spectra. Figures 13 and 14 show the effect of bleaching with

FIGURE 13

Optical absorption spectra of irradiated LiF measured with [011]
polarized light at 300°K before and after an optical bleach with
unpolarized light at 300°K. Curve (a) is the optical absorption
spectrum before the bleach. Curve (b) is the optical absorption
spectrum after a 930 min. bleach at 254 nm. Absorbed Dose –
0.12 Mrad

FIGURE 14

Optical absorption spectra of irradiated LiF measured with [0$\bar{1}$1] polarized light at 300°K before and after an optical bleach with unpolarized light at 300°K. Curve (a) is the optical absorption spectrum before the bleach. Curve (b) is the optical absorption spectrum after a 930 min. bleach at 254 nm. Absorbed Dose – 0.12 Mrad
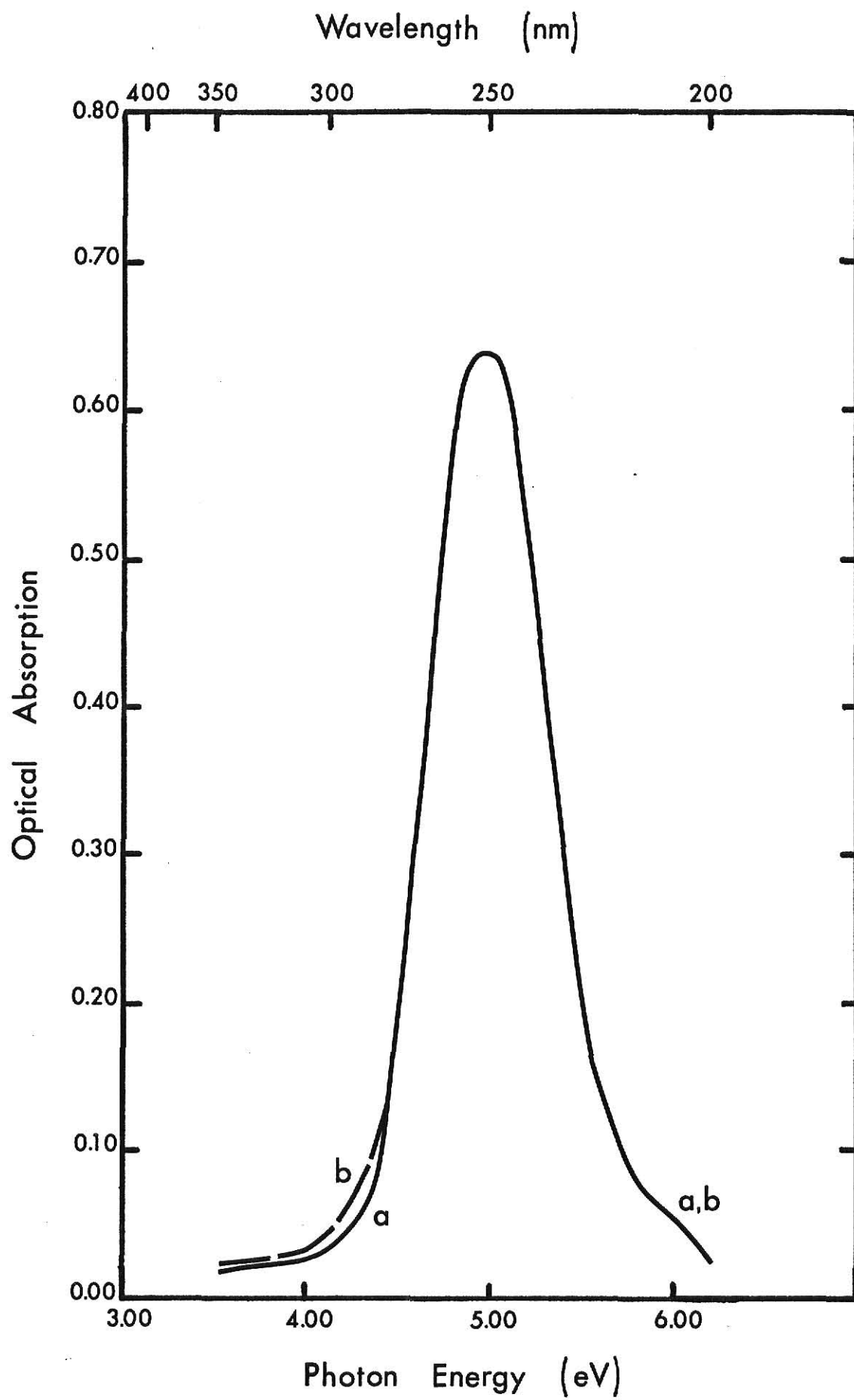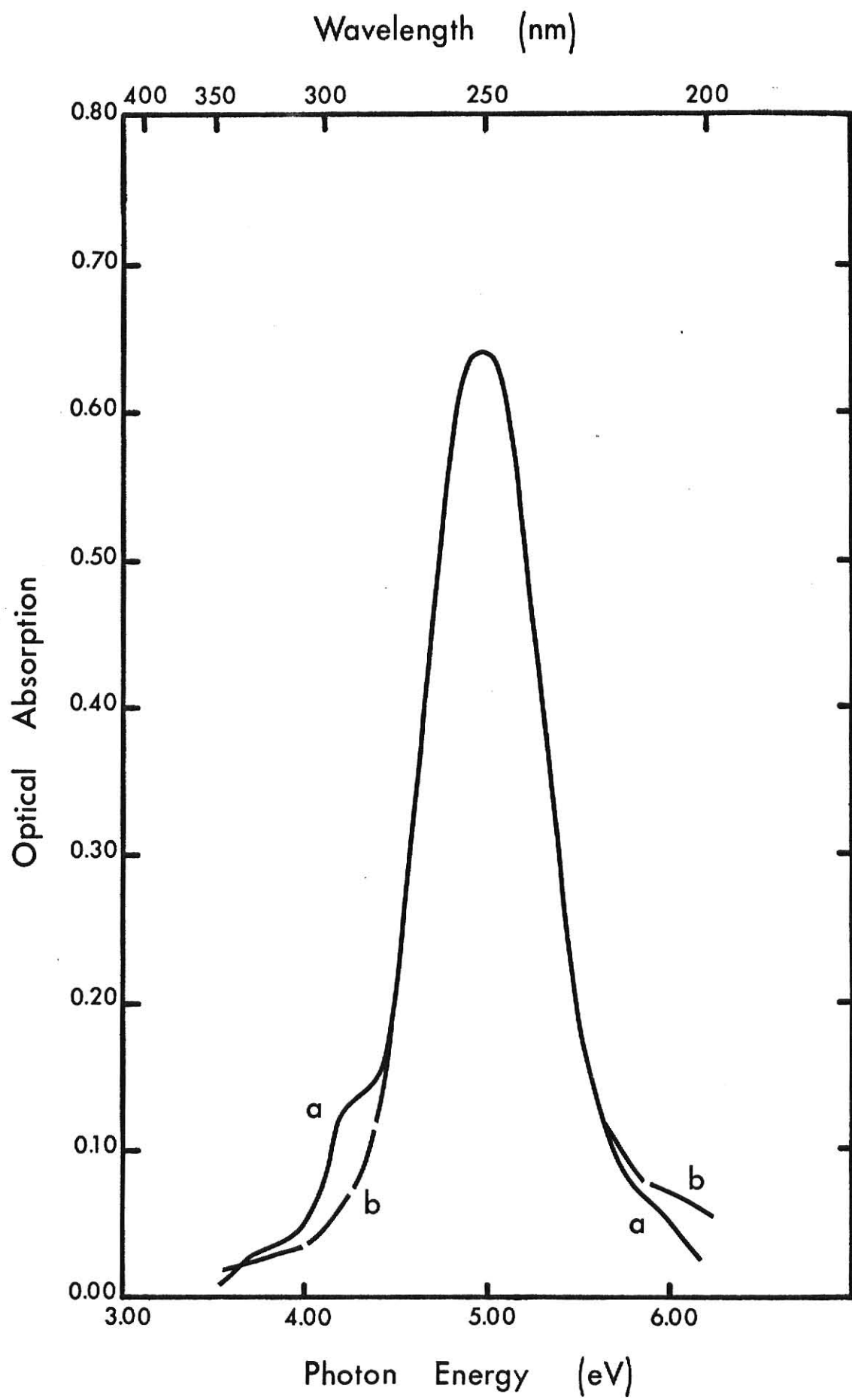
50

unpolarized light at 254 nm at 300°K for 930 minutes. Figure 13a is the optical absorption spectrum measured with [011] polarized light and Fig. 14a is the optical absorption spectrum measured with [0$\bar{1}$1] polarized light.before the optical bleach. Figures 13b and 14b are the respective optical absorption spectrum measured after the bleach. Comparing Figs. 13b and 14b, it is observed that the dichroism of the Y center has disappeared. The Y center optical absorption measured with [0$\bar{1}$1] polarized light has decreased and the Y center optical absorption measured with [011] polarized light has increased to make the optical absorption of the Y center equal for the two polarizations after the bleach. The decrease in the Y center optical absorption measured with [0$\bar{1}$1] polarized light is greater than the increase in the Y center optical absorption measured with [011] polarized light. This fact indicates that the optical bleach is also decreasing the population of the Y center. It is also observed that as a result of the bleach, the peak height of the F center absorption band does not change even though the wavelength of the bleaching light corresponds to the maximum of the F center absorption band. The fact that the peak height does not change can be understood since the ground state of the F center is approximately 8.5 eV below the conduction band minimum and cannot be optically bleached by a single-photon absorption process.[28,29]

The effect of bleaching on the optical absorption spectra with [011] polarized light at 244 nm at 90°K for 90 minutes is shown in Figs. 15 and 16 for [011] and [0$\bar{1}$1] polarized light, respectively. Figures 15a and 16a are the optical absorption spectra before the bleach and Figs. 15b and 16b are the optical absorption spectra after the bleach. The result of the

51

FIGURE 15

Optical absorption spectra of irradiated LiF measured with [011]
polarized light at 90°K before and after an optical bleach with
[011] polarized light at 90°K. Curve (a) is the optical absorption
spectrum before the bleach. Curve (b) is the optical absorption
spectrum after a 90 min. bleach at 244 nm. Absorbed Dose −
0.12 Mrad

FIGURE 16

Optical absorption spectra of irradiated LiF measured with [0$\bar{1}$1] polarized light at 90°K before and after an optical bleach with [011] polarized light at 90°K. Curve (a) is the optical absorption spectrum before the bleach. Curve (b) is the optical absorption spectrum after a 90 min. bleach at 244 nm. Absorbed Dose – 0.12 Mrad
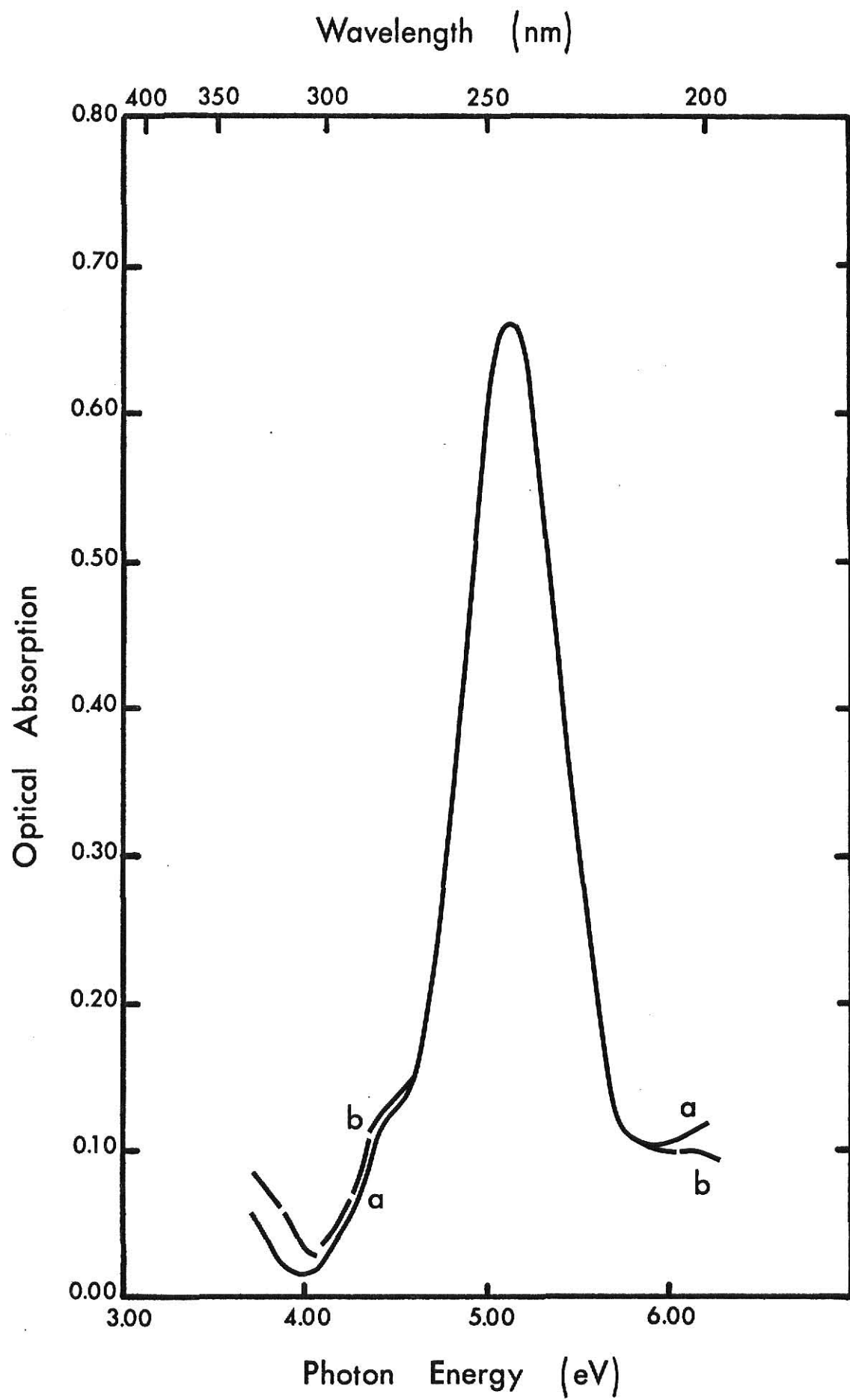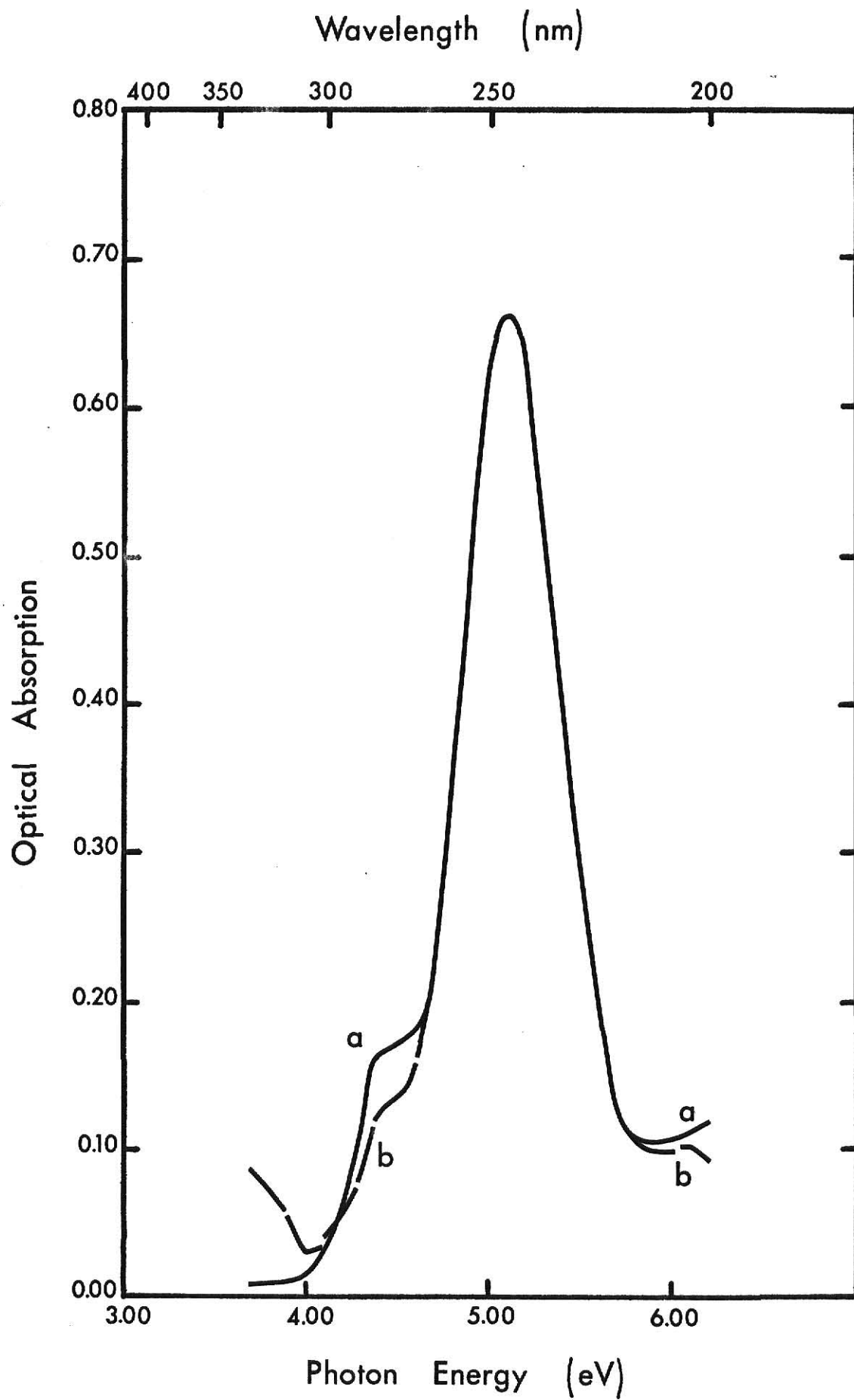
optical bleach with [011] polarized light is the same as that observed for
unpolarized light. The dichroism of the Y center has disappeared and the
Y center optical absorption for the two polarizations is equal after the
optical bleach.

The fact that the Y center optical absorption is equal for [011] and
[0$\bar{1}$1] polarized light after the bleach indicates that the Y center reoriented
itself so that the concentrations of the defect are equal for the two
polarizations. The mechanism of the reorientation is not clear. There are
examples of other defect centers, M centers and V_K centers, that can
reorient themselves upon the absorption of a photon. Schneider[38] proposed
the following mechanism for reorientation of the M center. At low
temperatures, the absorption of a photon leads to the ionization of the M
center by ejecting an electron. The ionized center, known as the M^+
center, absorbs another photon and rotates to a new orientation in its
excited state before returning to the M^+ ground state. Capture of an
electron converts the M^+ center back into a reoriented M center. At
temperatures above 100°K, the absorption of a second photon is unnecessary
for the M center since the reorientation can be made by thermal excitation.
A similar reorientation mechanism for the V_K center is proposed by
Delbecq et al.[39]

The fact that the Y center absorption band can be optically bleached
with [011] polarized light and unpolarized light corresponding to the F
center absorption band maximum at 90°K and 300°K respectively may
give an indication about the structure of the Y center. The F
center is an isotropic center, so it can absorb any direction
of polarized light. When bleaching at 90°K with [011] polarized

56

light at 244 nm, it is observed that the Y center optical absorption measured with [0$\bar{1}$1] polarized light decreases (see Fig. 16). This indicates that the Y center has an optical transition associated with it that is an F center optical transition. The above observations suggest that the Y center is a perturbed F center.

Photoconductivity of Irradiated LiF with Unpolarized Light

Figure 17 shows the normalized photoconductivity excitation spectrum of LiF for unpolarized light at various temperatures after exposure to 0.86 Mrad of gamma radiation. The spectrum at 300°K consists of a prominent photocurrent peak at 4.46 eV. The increase in the photocurrent at higher photon energies may indicate the presence of another photocurrent peak. It is questionable as to how much of the photocurrent increase is real, because the intensity of the Xenon lamp decreases very rapidly in the region of the increase making the normalization difficult (see Appendix IV). Figure 17 also shows that the decrease in temperature from 300°K to 100°K shifts the peak position to higher energy, decreases the FWHM, increases the area under the photocurrent peak, and increases the peak height. The photocurrent peak exhibits qualitatively the same behavior as the F center absorption band for decreasing temperature (see Fig. 10), except for the increase in the area under the photocurrent peak.

The shift of the peak position to higher energy with decreasing temperature can be explained by the same arguments given for the shift of the optical absorption bands (see Section-Optical Absorption of Irradiated LiF). Figure 18 shows how the peak position of the photocurrent peak at 4.46 eV at 300°K varies with decreasing temperature. The general

57

FIGURE 17

Normalized photoconductivity excitation spectra measured at
100°K, 214°K and 300°K. Curves (a), (b) and (c) are the
normalized photoconductivity excitation spectra measured
at temperatures of 300°K, 214°K and 100°K, respectively.
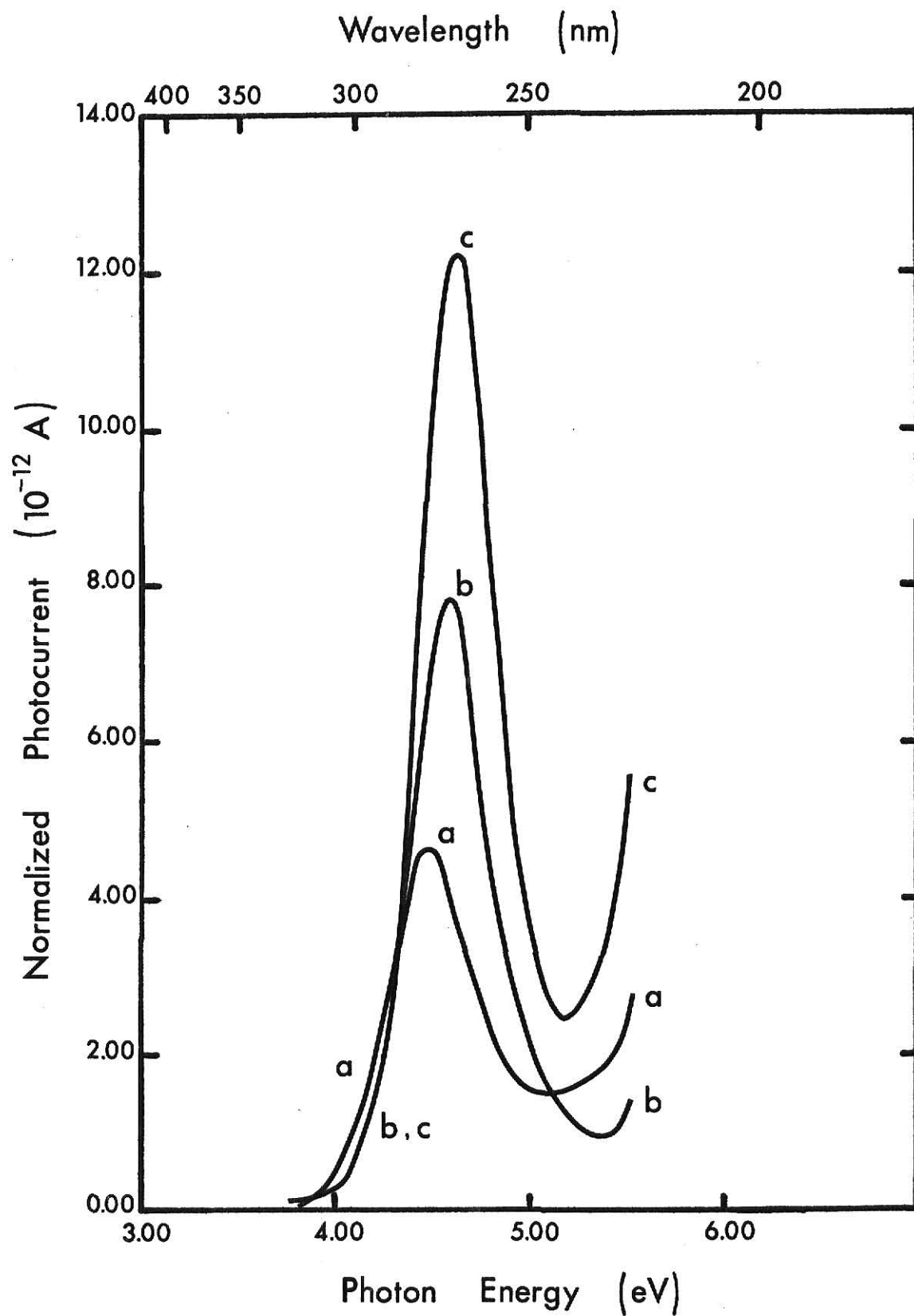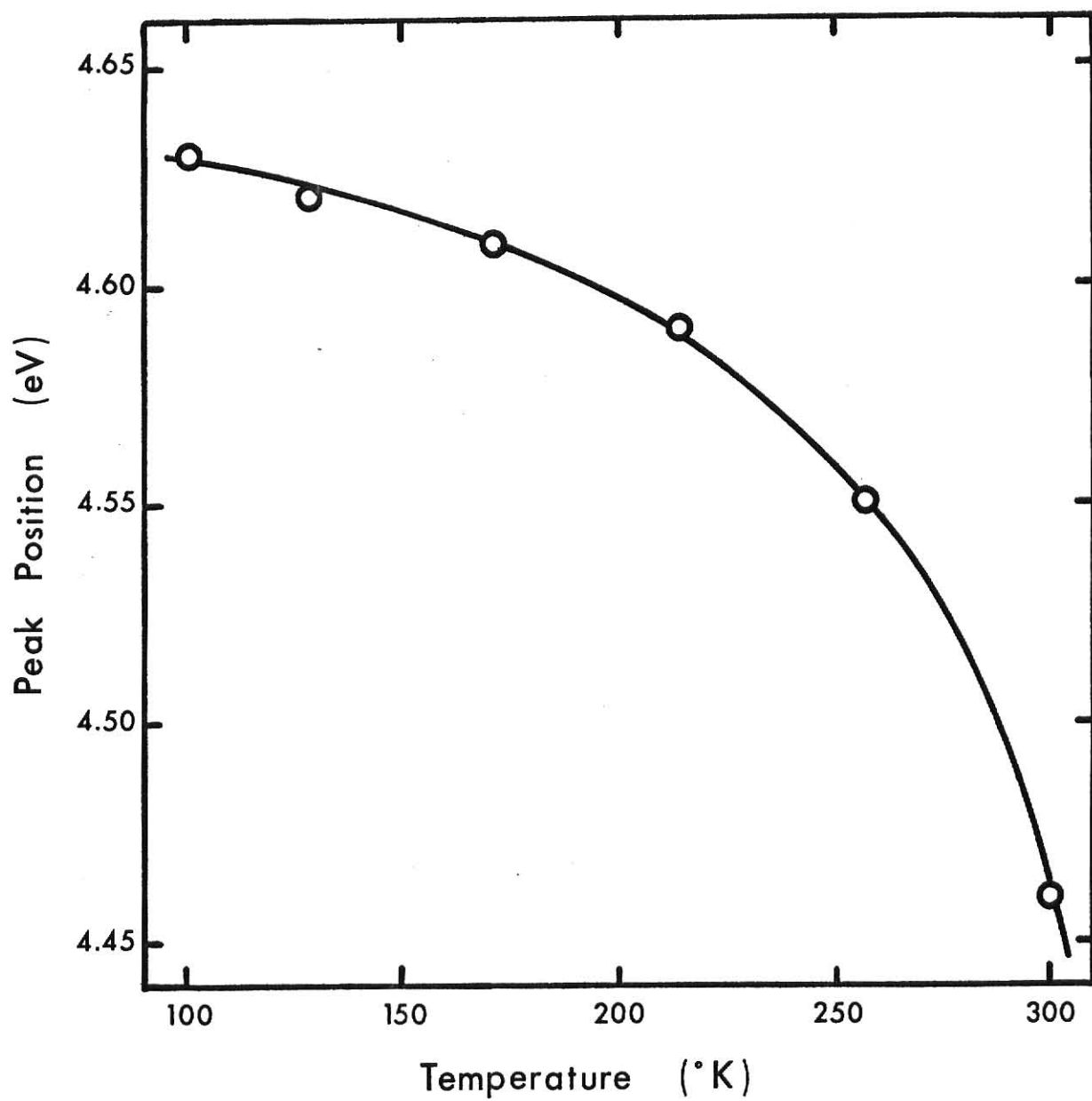Absorbed Dose - 0.86 Mrad.

59

FIGURE 18

Temperature dependence of the peak position of the 4.46 eV,

at 300°K, photocurrent peak

shape of the curve is the same as that observed for the temperature depen-
dence of the peak position of the F center absorption band in several of
the alkali halides.[35]

Figure 19 shows how the FWHM of the photocurrent peak varies with tempera-
ture. The FWHM of the photocurrent peak follows qualitatively the same temperatur
dependence as the FWHM of the F center absorption band in LiF.[35] Figure 19
also shows the best curve fit to the experimental points using the equation[4,8,35]

$$W = W_o \ \left[\coth\left(\frac{h\nu_g}{2kT}\right) \right]^{1/2} \ , \qquad (7)$$

which relates the observed width of the absorption band W to W_o, the width
of the absorption band at 0°K; ν_g, the lattice frequency around the defect
at 0°K; and T, the temperature of the observed bandwidth. W_o is determined
by extrapolating the data in Fig. 19 to 0°K and is 0.46 eV. Using Eq. 7,
ν_g is determined to be 1.05×10^{13} sec^{-1}. It should be pointed out that
Eq. 7 is derived to explain the temperature dependence of the width of an
optical absorption band, but it also can be applied to explain the
temperature dependence of the width of a photocurrent peak. The only
difference between an optical absorption measurement and a photocurrent
measurement is that in a photocurrent measurement the free charge carriers
have a drift velocity in a preferred direction because of the applied
electric field. The applied electric field should be small enough so
that the quantum efficiency for production of free charge carriers, the
retrapping rate and the recombination rate should remain relatively unchanged.

Applying the particle-in-a-box model of the F center, the width of
the absorption band is due to a variation in the amplitude of the thermal

FIGURE 19

Temperature dependence of the FWHM of the 4.46 eV, at 300°K,
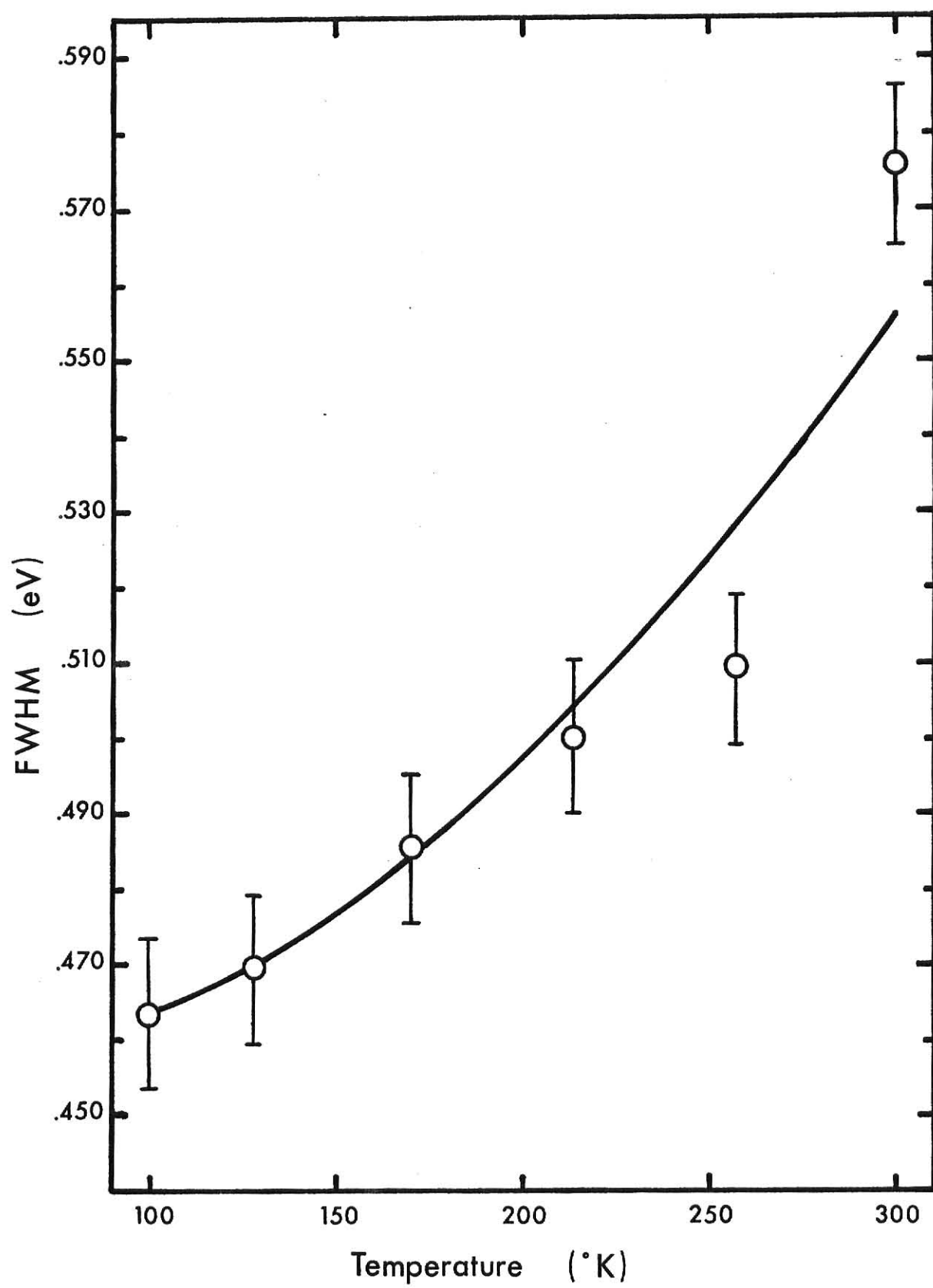
photocurrent peak

vibration of the Li^{+1} ions, surrounding the negative ion vacancy, about their zero-point position. The width of a photocurrent peak should have the same temperature dependence as the width of an optical absorption band. The width of the F center absorption band is 0.43 eV[35] and the width of the Y center photocurrent peak is 0.46 eV. Comparing the width of the F center optical absorption band in LiF at 0°K to the calculated width of the Y center photocurrent peak at 0°K, it is observed that they are essentially the same. This also supports the idea that the Y center is a perturbed F center.

The increase in the peak height and an increase in the area under the photocurrent peak with decreasing temperature, see Fig. 17, can be understood by examining the terms that contribute to the conductivity. The conductivity may change due to a change in the density of free charge carriers. The density of free carriers can be changed, for steady illumination, by a change in the production rate of the free carriers or a change in the mean lifetime of the carrier.

It is known that the quantum efficiency for the production of free charge carriers varies slowly with decreasing temperature until a temperature characteristic of the alkali halide is reached. Below this temperature the quantum efficiency decreases rapidly.[3,4,7,15,16] This temperature is not known for LiF, but the fact that the peak height and the area under the photocurrent peak increase with decreasing temperature indicate that this temperature has not been reached. Thus a change in the production rate of free carriers does not account for the observed changes in the peak height and area under the photocurrent peak with decreasing temperature.

The other contribution to the free charge carrier density is a change in the mean lifetime of a charge carrier. The mean lifetime will depend

on the various mechanisms which govern the rates of carrier removal from and emission into the conduction band and how these mechanisms vary with temperature. The fact that the area under the photocurrent peak increases with decreasing temperature indicates that the mechanisms governing the removal of free carriers from the conduction band have changed in such a way as to increase the carrier lifetime. The specifics of the change are not known.

Finally, the conductivity may change due to a change in mobility. It is observed that the mobility of free charge carriers increases with decreasing temperature. This is because the mobility is limited by scattering from optical phonons at high temperatures while scattering from impurities limit the mobility at low temperature.[3,4,15,26,27] The increased mobility will allow a larger number of free charge carriers to pass through a given area per unit time thus increasing the photogenerated current.

Photoconductivity of Irradiated LiF with [011] and [0$\bar{1}$1] Polarized Light

The Y center absorption band occurs at approximately the same energy as the 4.46 eV photocurrent peak which indicates they are produced by the same defect, the Y center. Thus the photocurrent spectrum was observed with [011] and [0$\bar{1}$1] polarized light at 300°K to see if the dichroism of the Y center absorption band was present in the Y center photocurrent peak. No dichroism was observed. The fact that no dichroism was observed would indicate that the applied electric field has somehow caused a re-orientation of the Y center. The mechanism for the reorientation is not known but it may be associated with a large dark current that is observed at room temperature.

Effect of Optical Bleaching on the Photoconductivity Excitation Spectrum

The effect of optical bleaching with either unpolarized light or [011] polarized light at 254 nm at 300°K was observed by the changes in the photoconductivity excitation spectrum. The sample was not biased when the bleaching was performed. The result of the optical bleach was the same for the unpolarized light and [011] polarized light. The peak height of the Y center photocurrent peak decreased with increasing bleaching time. After the desired bleaching time had passed, the photocurrent spectrum was measured over a period of time to see if the peak would approach its original height. No increase was observed. This indicates that the electrons freed from the Y center during the optical bleach have become trapped at some other electron trap or have undergone recombination with a hole.

Effect of Decreasing Temperature on the Dark Current of Irradiated LiF

When an electric field is applied to a sample, a dark current varying from one to two orders of magnitude smaller than the peak photocurrent is observed at 300°K. As the temperature is decreased, the magnitude of the dark current decreases to the point that it is in the range of the noise level of the equipment, 10^{-16} amps.

In alkali halides, impurities, Frenkel defects and Schottky defects are mobile and under the influence of an applied electric field they will move with their respective mobilities.[7,10,26] This motion will produce a current referred to as ionic current.

Since the motion of any defect, ion or atom in a solid is governed by the probability that the defect can move to an adjacent site, the activation energy for motion of the defect must be small enough so that

67

ILLEGIBLE DOCUMENT

THE FOLLOWING DOCUMENT(S) IS OF POOR LEGIBILITY IN THE ORIGINAL

THIS IS THE BEST COPY AVAILABLE

movement to an adjacent site is possible. The probability P of a defect moving is governed by the equation[7,10,36]

$$P = \nu_0 e^{-E_A/kT} \quad , \tag{8}$$

where ν_0 is the jump frequency and is on the order of 10^{13} Hz, E_A is the activation energy of the process, k is Boltzmann constant and T is the temperature.

The energy of activation for motion of a Frenkel defect in LiF is 1.3 eV,[20] compared to 1.9 eV[20] for the energy of activation for motion of a Schottky defect. These energies indicate that at 300°K these defects could move producing the observed dark current.[20,40] As the temperature decreases, so does the probability for movement of these defect decreases, thus lowering the current.

A Model for the Y Center

Since the Y center is responsible for the optical absorption band on the low energy side of the F center and the photocurrent peak at 4.46 eV, a model will have to be able to explain the observed data for the optical absorption and photocurrent measurements.

A possible structure of the Y center can be proposed by considering the following observations:

(1) The variation of the Y center absorption band peak height from sample to sample suggests that the Y center is associated with an impurity atom or ion.

(2) The optical absorption band maximum of the Y center occurs around 4.4 eV, approximately 0.6 eV below the maximum of the

68

F center absorption band at 5.0 eV.

(3) The Y center absorption band can be optically bleached with
F center absorption band light that is either unpolarized, at
254 nm at 300°K, or [011] polarized light, at 244 nm at 90°K.

(4) The FWHM at 0°K of the F center absorption band is 0.43 eV.[35]
This is compared to the FWHM of the photocurrent peak of the
Y center of 0.46 eV at 0°K.

(5) The Y center absorption band exhibits dichroism with respect
to [011] and [0$\bar{1}$1] polarized light.

(6) No dichroism is observed in the Y center photocurrent peaks
with respect to [011] and [0$\bar{1}$1] polarized light.

The observations above suggest that the Y center may be a perturbed
F center. Three possible perturbed F centers are shown in Fig. 20. They
are,

(a) a substitutional impurity ion on a Li^{+1} site,

(b) a substitutional impurity ion on a F^{-1} site,

(c) and an interstitial positive ion impurity.

The substitutional impurity on a Li^{+1} site, as in Fig. 20a, would lie
in the [010] or the [001] direction. This perturbation on the F center
would not produce the observed dichroism for the [011] and [0$\bar{1}$1] polarized
light. Thus it will be excluded as a possible model.

A substitutional impurity on a F^{-1} site, as in Fig. 20b, could produce
the observed dichroism. Optical bleaching with [011] polarized light at
90°K removes the dichroism, which implies a reorientation of the Y center.
This reorientation would require the vacancy to diffuse two negative ion

69

FIGURE 20

Three possible models of the Y center:

(a) Substitional positive ion impurity on a Li^{+1} site as a
    nearest neighbor to an F center

(b) Substitional negative ion impurity on a F^{-1} site adjacent
    to an F center

(c) Interstitial positive ion impurity adjacent to an F center.
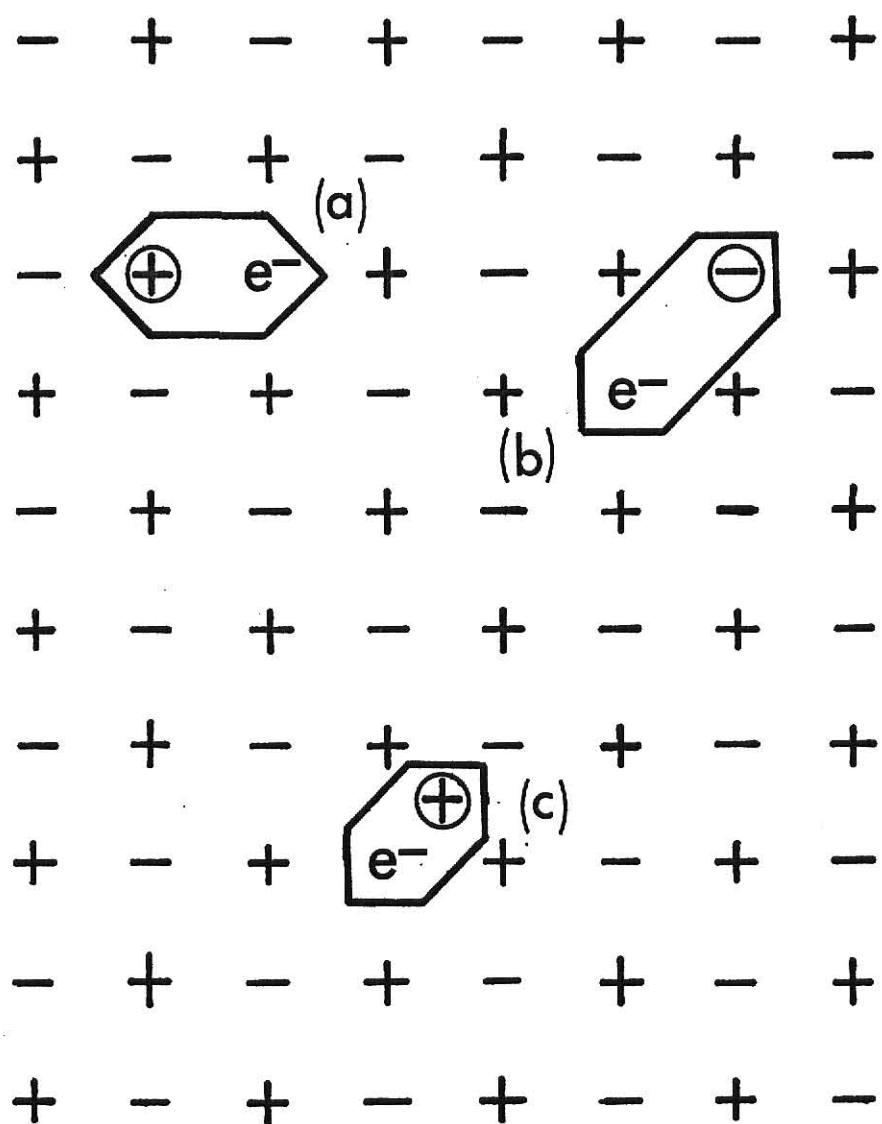
sites after the electron was ejected from the center. The activation energy

for the motion of a negative ion vacancy is 1.1 eV in LiF.[40] Thus at 90°K

the process of reorientation by diffusion has a very small probability of

occurring. There is also the possibility that the defect could reorient

by the absorption of a photon, thus showing the observed bleaching behavior.

Recent work[37] has shown the Y center absorption band is present without any

negative ion impurities present in the sample. This fact eliminates the

substitutional impurity on a F^{-1} site as a possible model of the Y center.

The interstitial positive ion impurity, shown in Fig. 20c, could

produce the observed dichroism. Reorientation of this defect would require

the ejection of the electron from the defect upon absorption of a photon

and thermal diffusion of the interstitial to a neighboring interstitial

site. The energy of activation for motion of positive ion interstitials

in several of the alkali halides is on the order of 0.10 eV.[20,26] By

analogy the energy of activation for the motion of positive ion inter-

stitials in LiF should be of the same magnitude. An energy of this order

would make thermal diffusion of the positive ion interstitial possible at

90°K. Also, as is the case with other defects[38,39], the reorientation

could be possible by absorption of a photon by the defect in the ionized

state.

The fact that the photocurrent spectrum does not possess dichroic

behavior with respect to [011] and [0$\bar{1}$1] polarized light can be understood

only qualitatively. The application of the applied electric field might

be able to reorient the Y center. The mechanism for reorientation may

be associated with the large dark current that is observed at room

temperature, but specifics are not clear at this point.

There is also some indication as to where the energy levels of the Y center are relative to the conduction band minimum. The fact that the Y center photocurrent peak is observed at temperatures down to 85°K indicates that the excited state of the Y center is close enough to the conduction band to allow thermal ionization and ejection of the electron into the conduction band. The close proximity of the excited state of the Y center to the conduction band is also supported by the fact that the Y center absorption band is optically bleached at 90°K.

V. SUMMARY AND CONCLUSIONS

The results of the experiments with [011] and [0$\bar{1}$1] polarized light on the optical absorption spectrum of irradiated LiF indicate there is an unresolved, dichroic absorption band on the low-energy side of the F center absorption band (5.0 eV). The dichroic absorption band maximum occurs at ∿4.4 eV and is labeled the Y center absorption band. The dichroism indicates that the concentration of the Y centers oriented in the [0$\bar{1}$1] direction is larger than the concentration of Y centers oriented in the [011] direction. The mechanism for producing the dichroism in the Y center absorption band is not known.

The effect of optical bleaching with unpolarized light at 254 nm at 300°K and [011] polarized light at 244 nm at 90°K is observed by changes in the optical absorption spectra. The result of optical bleaching is observed to be the same for unpolarized light as it is for [011] polarized light. The optical absorption of the Y center measured with [0$\bar{1}$1] polarized light decreases and the optical absorption of the Y center measured with [011] polarized light increases to the point that the optical absorption for the two polarizations is equal after the bleach. It is also observed that the decrease in the optical absorption of the Y center measured with [0$\bar{1}$1] polarized light is larger than the increase in the optical absorption of the Y center measured with [011] polarized light. This indicates that the population of the Y center is decreasing as a result of the optical bleach. The fact that the optical absorption of the Y center measured with [011] and [0$\bar{1}$1] polarized light is equal after the optical bleach indicates that the Y center has reoriented.

Photoconductivity excitation spectra are measured with unpolarized light at temperatures from 85°K to 300°K. A photocurrent peak is observed at 4.46 eV at 300°K. It is observed that the peak position of the photo-current peak shifts to higher energy, the FWHM of photocurrent peak decreases, the peak height of the photocurrent peak increases and the area under the photocurrent peak increases with decreasing temperature. The shift of the peak position to higher energy, increase of the peak height and decrease in the FWHM of the photocurrent peak exhibit qualitatively the same temperature dependence as observed for the F center absorption band. The shift of the peak position and decrease in the FWHM is qualitatively explained by the particle-in-a-box model of a defect. The increase in the peak height and area under the photocurrent peak is attributed to an increase in the mobility and mean lifetime of the electron with decreasing temperature.

Since the photocurrent peak at 4.46 eV is attributed to the same defect as that which produces the absorption band at ~4.4 eV, the photoconductivity excitation spectrum is measured with [011] and [0$\bar{1}$1] polarized light at 300°K to determine if the Y center photocurrent peak is dichroic. No dichroic behavior is observed. The reason no dichroism is observed, is believed to stem from the applied electric field causing reorientation of the Y center.

A dark current on the order of 10^{-15} amps is observed at 300°K. The magnitude of the dark current decreases with decreasing temperature. The dark current is attributed to motion of Frenkel and Schottky defects under the influence of the applied electric field.

Based on the optical absorption and photoconductivity measurements, a model is proposed for the structure of the Y center. The model involves an interstitial positive ion impurity adjacent to an F center.

Areas of further study should include dependence of absorption band maxima and photoconductivity of the Y center on the concentation of impurities. Photoconductivity measurements should be extended below 200 nm in the hopes of observing other possible photocurrent peaks associated with the Y center. The measurement of the optical absorption spectra and the photoconductivity should be extended to lower temperatures to determine the energy levels of the Y center relative to the conduction band minimum. ESR measurements would be useful in determining the structure of the Y center.

VI.   REFERENCES

1.   C. Doelter, "Colorations Obtained Under the Influence of Radium Ray," Lab. Mineral., University of Vienna, Radium 7, 58 (1911).

2.   S. C. Lind and D. C. Bardwell, "Coloring and Thermophosphorescence Produced in Transparent Minerals and Gems by Radium Radiation," J. Franklin Inst. 196, 357 (1924); Am. Mineralogist 8, 171 (1923).

3.   J. J. Markham, F-centers in Alkali Halides (Academic Press Inc., New York, 1966).

4.   J. H. Schulman and W. D. Compton, Color Centers in Solids (Pergamon Press, New York, 1962).

5.   R. W. Pohl, "Electron Conductivity and Photochemical Processes in Alkali Halides," Proc. Phys. Soc. 49, (extra part), 3 (1937).

6.   K. Przibram, Irradiation Colors and Luminescence (Pergamon Press, London, 1956).

7.   R. W. Gurney and N. F. Mott, Electronic Processes in Ionic Crystals (Clarendon Press, Oxford, 1940).

8.   W. B. Fowler (Ed.), Physics of Color Centers (Academic Press Inc., New York, 1968).

9.   P. Görlich, Photoconductivity in Solids (Dover Publications Inc., New York, 1967).

10.   F. Seitz, The Modern Theory of Solids (McGraw-Hill Book Co., New York, 1940).

11.   M. P. Givens and A. Milgram, "Extreme Ultraviolet Absorption by Lithium Fluoride," Phys. Rev. 125, 1506 (1962).

12. H. Pick, "Color Centers in Alkali Halides," Nuovo Cimeto VII (Ser. X), No. 2, Suppl., 498 (1958).

13. G. Woffram, "Photoconductivity of Z_2 Centers in KCℓ: Sr Crystals," Phys. Status Solidi $\underline{28}$, K11-13 (1968).

14. R. Crandall and M. Mikkor, "Photoconductivity of KBr Containing F Centers," Phys. Rev. $\underline{138}$, A1247 (1965).

15. H. Kanzaki and F. Nakazawa, "Low Temperature Photoconductivity of F Centers in KCℓ," J. Phys. Soc. Japan $\underline{22}$, 844 (1967).

16. N. Inchauspe, "Photoconduction in KCℓ and KI Containing F Centers," Phys. Rev. $\underline{106}$, 898 (1957).

17. J. J. Oberly, "Photoconductivity of Trapped Electrons in KBr Crystals at Room Temperature," Phys. Rev. $\underline{84}$, 1257 (1951).

18. G. R. Cole and R. J. Friauf, "Photoconductivity of Z bands in KCℓ," Phys. Rev. $\underline{107}$, 387 (1957).

19. R. H. Bube, Photoconductivity of Solids (John Wiley and Sons, Inc., New York, 1960).

20. J. H. Crawford and L. N. Slifkin (Ed.), Point Defects in Solids (Plenum Press, New York, 1972), Vol. I, General and Ionic Crystals.

21. S. K. Metha, Study of Optical Absorption Bands Responsible for Thermoluminescence of LiF: Mg, Ph.D. Dissertation, Kansas State University, Department of Nuclear Engineering (1972), (unpublished).

22. E. N. Nelson, Area Photoconductivity in Lithium Fluoride, M.S. Thesis, Kansas State University, Department of Nuclear Engineering (1974), (unpublished).

23. A. Rose, Concepts in Photoconductivity and Allied Problems (Interscience Publishers, New York, 1963).

24. T. S. Moss, <u>Photoconductivity in the Elements</u> (Academic Press Inc., New York, 1952).

25. P. D. Townsend and J. C. Kelley, <u>Color Centers and Imperfections in Insulators and Semiconductors</u> (Crane, Russak and Co., New York, 1973).

26. C. Kittel, <u>Introduction to Solid State Physics</u> (John Wiley and Sons, Inc., New York, 1971), 4th ed.

27. R. K. Ahrenkiel and F. C. Brown, "Electron Hall Mobility in the Alkali Halides," Phys. Rev. <u>136</u>, A223 (1964).

28. J. A. Knapp, G. J. Lapeyne and P. L. Gobby, "Photoemission Study of Polycrystalline LiF," Bull. Am. Phys. Soc., Ser. II, <u>20</u>, No. 3, 474 (1975).

29. D. S. Choo and G. W. Pratt, "Investigation of Isoelectronic Traps and F Centers by the X $\propto$ Cluster Method," Bull. Am. Phys. Soc., Ser. II, <u>20</u>, No. 3, 468 (1975).

30. M. Kaiserudden, <u>Effects of Very High Dose Rates on the Response of LiF Thermoluminescent Dosimeters</u>, M.S. Thesis, Kansas State University, Department of Nuclear Engineering (1968), (unpublished).

31. E. Burstein and J. J. Oberly, "Optical Properties of F Centers at Liquid Helium Temperatures," National Bureau of Standards Circular <u>519</u>, 285 (1951).

32. C. Z. van Doorn, "Color Centers in KCℓ," Philips Res. Rep. Supplement <u>4</u> (June 1962).

33. T. Inui and Y. Uemura, "Theory of Color Centers in Ionic Crystals, II The Temperature Dependence of F-bands in Alkali Halides, Prog. Theor. Phys. <u>5</u>, 395 (1950).

34. D. E. Gray (Coord. Ed.), <u>American Institute of Physics Handbook</u> (McGraw-Hill Book Co., New York, 1972), 3rd ed.

35. G. A. Russell and C. C. Klick, "Configuration Coordinate Curves for F Centers in Alkali Halides," Phys. Rev. <u>101</u>, 1473 (1956).

36. P. Warmeck, "LiF Color Center Formation and UV Transmission Losses From Argon and Hydrogen Discharges," J. Opt. Soc. Am. <u>55</u>, 921 (1965).

37. M. Richter, private communication.

38. I. Schneider, "Reorientation of M Centers in KCℓ," Phys. Rev. Lett. <u>24</u>, 1296 (1970).

39. C. J. Delbecq, W. Hayes and P. H. Yuster, "Absorption Spectra of F_2^-, $Cℓ_2^-$, Br_2^- and I_2^- in the Alkali Halides," Phys. Rev. <u>121</u>, 1043 (1961).

40. T. G. Stoebe and P. L. Pratt, "Ionic Conductivity and Diffusivity in LiF," Proc. Brit. Ceram. Soc. <u>9</u>, 181 (1967).

APPENDIX I

Neutron Activation Analysis of LiF Samples

A qualitative neutron activation analysis was run on two LiF samples
to determine what impurities were present. The samples were individually
irradiated in polyethylene vials in the Triga Mark II Reactor located in
the Nuclear Engineering Department. The reactor was operated at 100
kilowatts, which corresponds to a neutron flux of approximately 7.2×10^{11} n/cm$^2\cdot$sec
The samples were irradiated, one at a time, for four minutes at the
above flux. After the irradiation, the sample was removed from the reactor
specimen rack and since the polyethylene vial had also become activated,
the sample was placed in an unirradiated polyethylene vial. The vial
was then placed on the Ge(Li) detector that was part of the Northern
Scientific Analyzer System. Data was collected for two consecutive periods
of 256 seconds. After the sample data was collected, the calibration of
the analyzer was determined by Cobalt-60 and Cesium-137 gamma-rays. The
impurities that Harshaw Corporation said were possibly present were: Aℓ,
Ca, Fe and Mg with concentrations of 1-3 ppm. The impurities found were:
Aℓ, Na and Cℓ with concentrations of the same order as shown.

APPENDIX II

Determination of the Photon Flux Used for the Bleaching Experiments

The determination of the photon flux of a lamp is formulated in the following manner. By definition,

$$Intensity = Average\ Power/Area \qquad (1)$$

and

$$Intensity = (Number\ of\ photons/unit\ area \cdot unit\ time)$$
$$X(Energy\ of\ a\ single\ photon) \qquad (2)$$

Combining Equations 1 and 2 and solving for the photon flux, N, gives,

$$N = \frac{I}{E} = \frac{P}{E} \cdot \frac{1}{A} \qquad , \qquad (3)$$

where

I = intensity of the light,

E = energy of a single photon in eV,

A = area of illumination in m^2,

P = power in watts, from Power Meter.

Values taken at 254 nm for the Xenon Lamp are:

$$E = 4.88 \text{ eV/photon}$$

$$A = 7.5 \times 10^{-5} \text{ m}^2$$

$$P = 5.4\mu v \cdot \frac{10\mu w}{1\mu v} = 54\mu w = 5.4 \times 10^{-5} \text{ watt.}$$

Substituting these values into Equation 3 gives,

$$N = 9.21 \times 10^{13} \text{ photons/cm}^2 \cdot \text{sec.}$$

This is the photon flux at the sample position for an area of one square centimeter. If one calculates the illumination of the 0.126 cm^2 hole in the biasing electrode, the number of photons incident on the crystal face per unit time is, 1.16×10^{13} photons/sec.

The same experiment was done using the Mercury Lamp as the light source. The values for an area of illumination of 1 cm^2 are; for 244 nm,

$$E = 5.08 \text{ eV/photon}$$

$$A = 5.35 \times 10^{-4} \text{ m}^2$$

$$P = 9.3\mu v \cdot \frac{10\mu w}{1\mu v} = 9.3 \times 10^{-5} \text{ watt}$$

which yields a photon flux, $N = 2.14 \times 10^{13}$ photons/cm^2·sec; for 254 nm,

$$E = 4.88 \text{ eV/photon}$$

$$A = 5.35 \times 10^{-4} \text{ m}^2$$

$$P = 11.2\mu v \cdot \frac{10\mu w}{1\mu v} = 1.12 \times 10^{-4} \text{ watt}$$

which yields a photon flux, $N = 2.68 \times 10^{13}$ photons/cm^2·sec.

Since some samples were bleached with light polarized in the [011] direction, a correction of these values must be made to account for the effect of the polarizer. The correction is simply the percent transmission of the polarizer at the two wavelengths. At 244 nm the percent transmission was 20.5% and at 254 nm the percent transmission of light polarized in the [011] direction was 23.2%. The corrected values are 4.39×10^{12} photons/sec at 244 nm and 6.22×10^{12} photons/sec at 254 nm.

APPENDIX III

Wavelength Calibration of Jarrell-Ash and Bausch Lomb Monochromators

The wavelength calibration of the Jarrell-Ash, Model 82-410, .25 Meter Ebert Monochromator and Bausch and Lomb 33-88-01 Grating Monochromator was determined by the experimental arrangement shown in Fig. 21.

A helium cadium laser, Model ML-442, made by Meterologic Inc. was used as the light source. The 442 nm laser line was used as one calibration wavelength for the Jarrell-Ash Monochromator. The other calibration wavelengths were the fluorescence lines of helium and cadium present in the laser channel. A front surface mirror was used to reflect the light from the channel onto the entrance slit of the monochromator. The light passing out the exit slit was detected by a Jarrell-Ash photomultiplier tube, Type 1P28, with a S5 response. The tube was biased at -750 volts with a Fluke High Voltage Power Supply, Model 415B. The output of the PM tube was monitored with a Keithley Picoammeter, Model 410A. The measured wavelengths and the actual wavelengths for the Jarrell-Ash and Bausch and Lomb Monochromators are shown in Fig. 22 and Fig. 23, respectively.

FIGURE 21

Experimental arrangement used for the wavelength calibration of the Jarrell-Ash and Bausch

and Lomb monochromators

He-Cd Laser

Front Surface Mirror

J-A or B-L Monochromator

1P28 Photomultiplier Tube & Mount

Fluke 415B High Voltage Supply
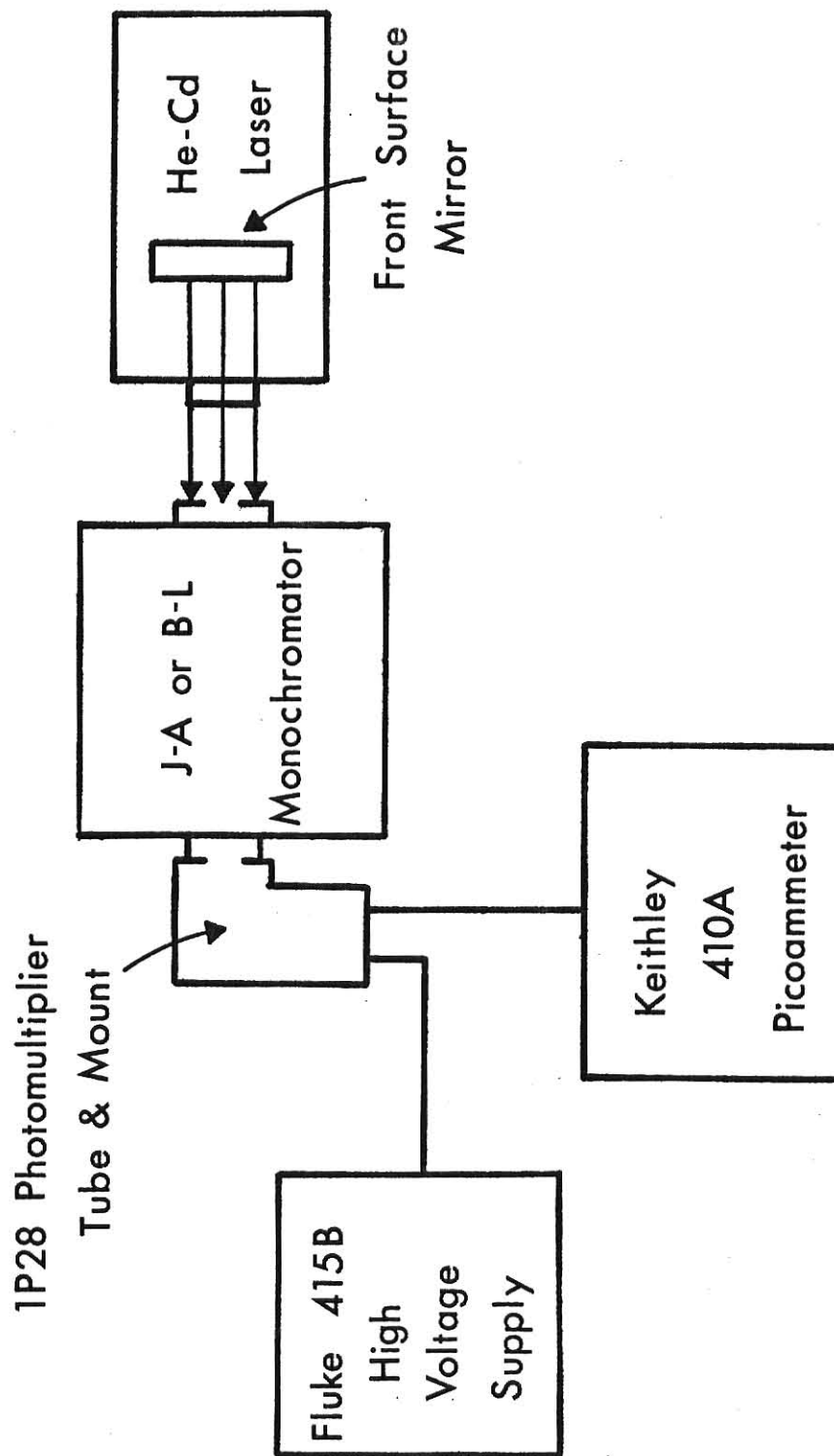
Keithley 410A Picoammeter

FIGURE 22

Wavelength calibration curve for the Jarrell-Ash monochromator
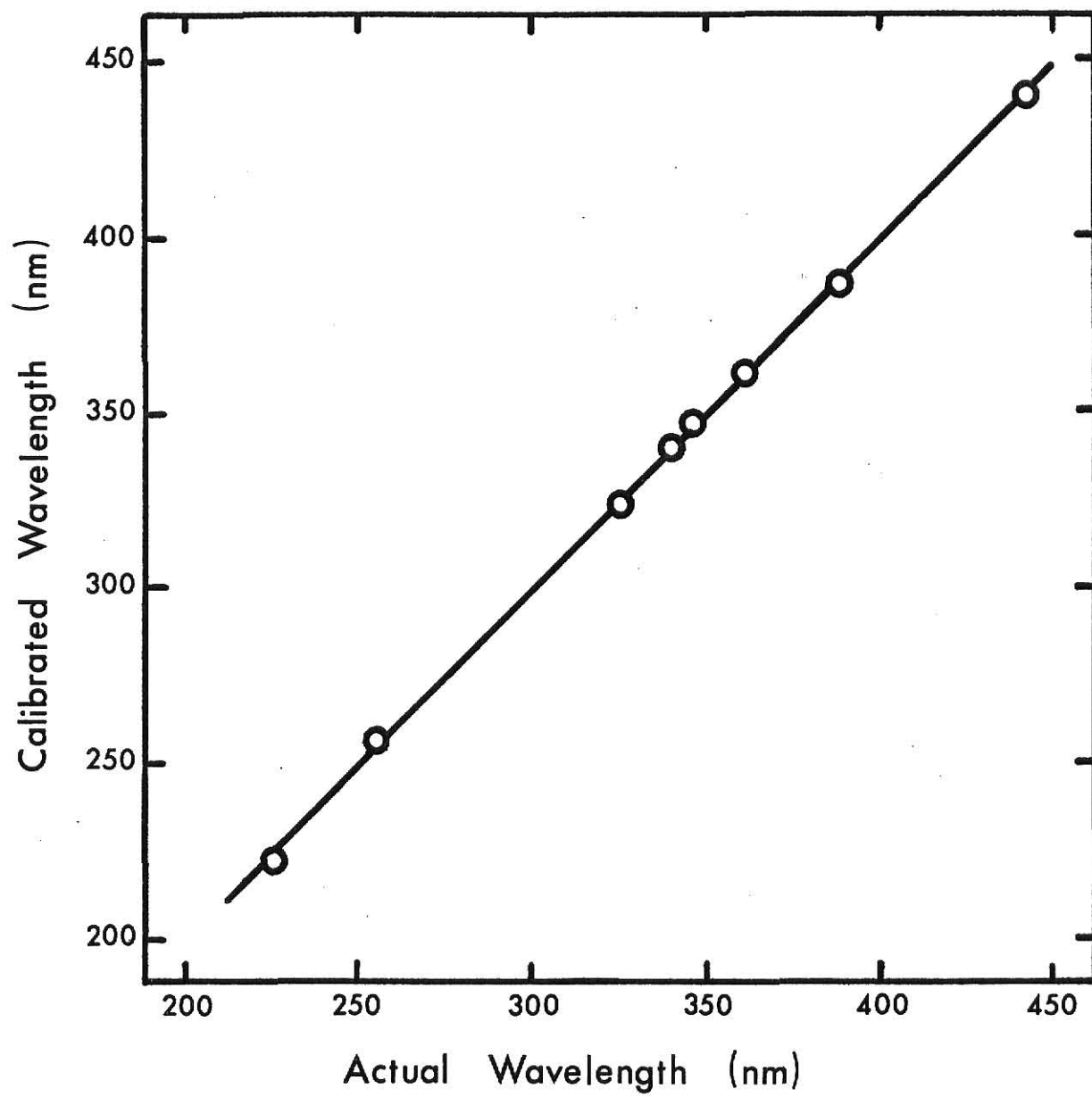The solid line represents a least-squares fit to the experimental
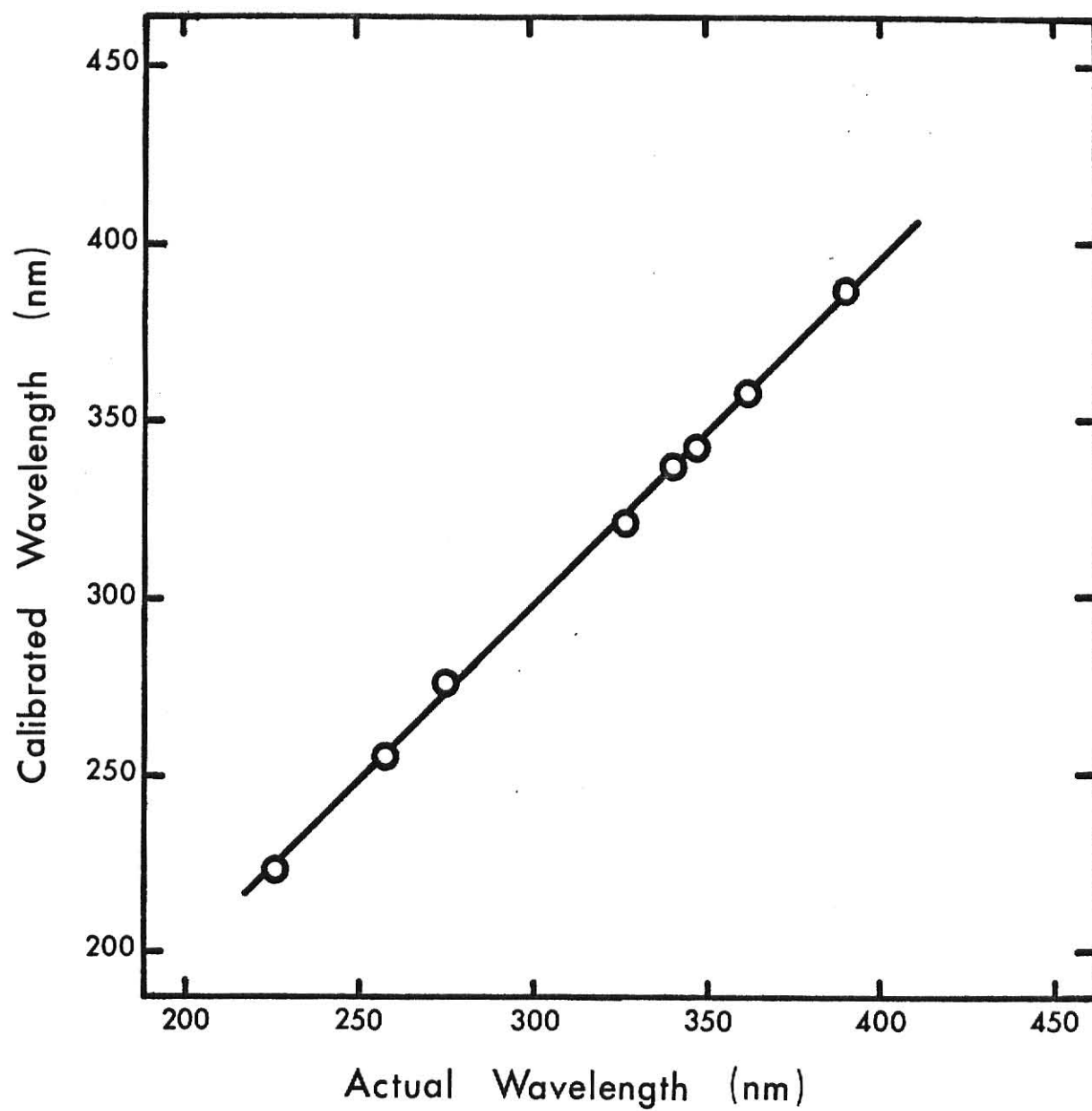data.

FIGURE 23

Wavelength calibration curve for the Bausch and Lomb

monochromator. The solid line represents a least-squares

fit to the experimental data.

APPENDIX IV

Determination of the Spectral Distribution of the Xenon Lamp

and Normalization of Photocurrents

The output of the Xenon Lamp is dependent upon the wavelength and this fact is reflected in the photoconductivity spectra that was observed. To normalize the photoconductivity spectra to a constant photon flux, the spectral distribution of the lamp must be determined at the sample position.
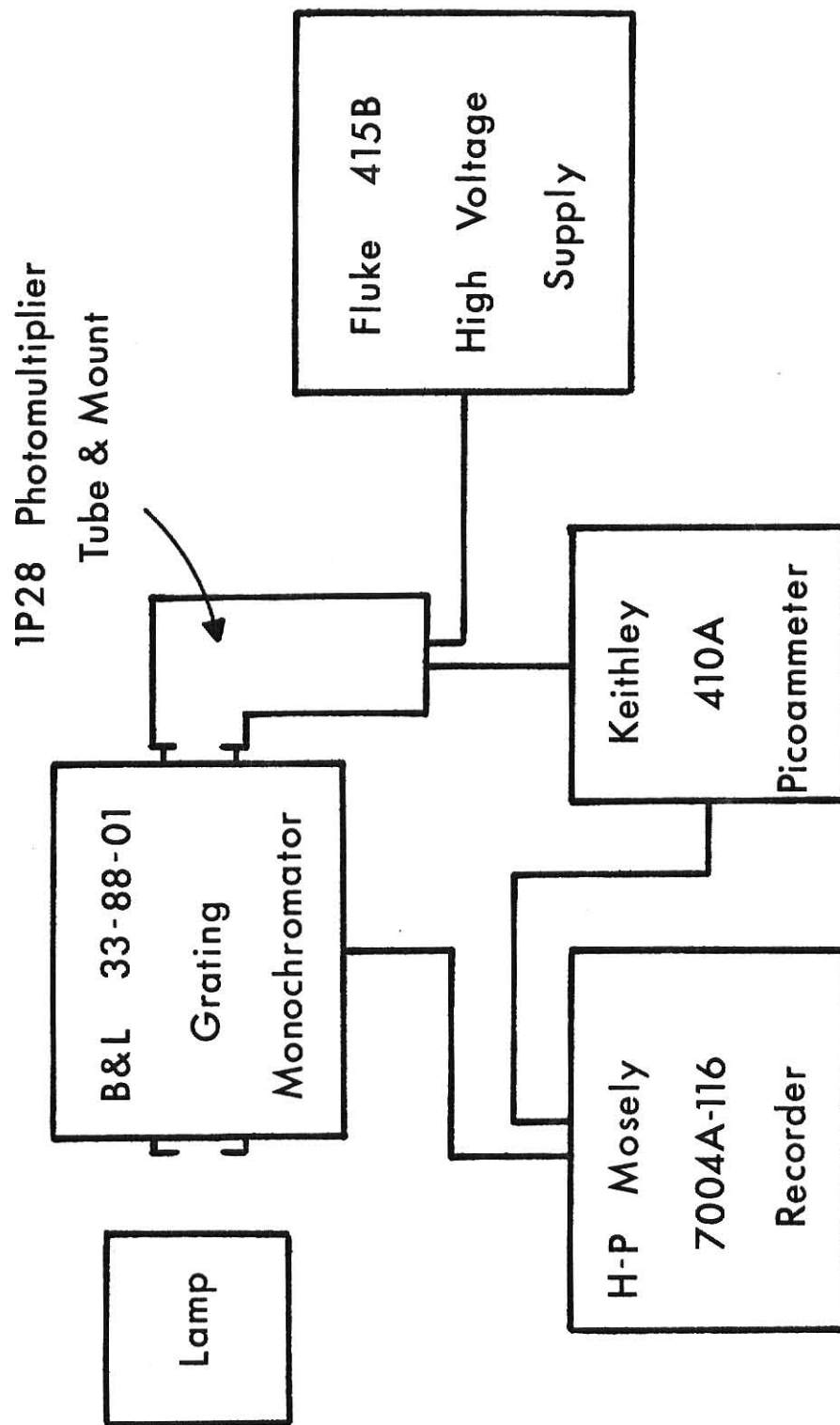
Figure 24 shows the experimental arrangement for determining the radiative power for the lamp. A Tungsten-Iodide Standard Lamp, Model L-101, and Power Supply, Model P-101, was used to determine the sensitivity of the Bausch and Lomb Monochromator and the Jarrell-Ash photomultiplier tube. The photocathode of the PM tube was at the same distance from the exit slit as a sample. The tube was biased at -750 volts with a Fluke High Voltage Power Supply, Model 415B. The output was read by a Keithley Picoammeter, Model 410A, and plotted versus wavelength on a Hewlett-Packard 7004A-116 X-Y Plotter. Both the Xenon Lamp and the Standard Lamp responses were determined by this method.

The sensitivity of the monochromator - PM-tube system, in milliamp/μwatt, was determined by measuring its response to the standard lamp. The power-spectral distribution for the standard lamp is given by,

$$I_{40} = \frac{\propto}{\lambda^5 (e^{\beta/\lambda} - 1)}$$

FIGURE 24

Experimental arrangement for the determination of the radiative power of the Xenon Lamp.

Lamp denotes either the Tungsten-Iodide Standard Lamp or the 150 watt Xenon Lamp.

1P28 Photomultiplier Tube & Mount

Fluke 415B High Voltage Supply

Keithley 410A Picoammeter

B&L 33-88-01 Grating Monochromator

H-P Mosely 7004A-116 Recorder

Lamp

where,

$$\alpha = 6.768 \times 10^{-18} \ \mu w \cdot cm^3 / 10\mathring{A}$$

$$\beta = 4.593 \times 10^{-4} \ cm$$

$$\lambda = \text{wavelength in cm}$$

$$I_{40} = \text{spectral radiance in } \mu w/cm^2 \cdot 10\mathring{A} \text{ at 40 cm from the entrance slit.}$$

The standard lamp was 15.4 cm from the entrance slit of the monochromator, so a correction to the spectral radiance must be made. This was done by,

$$I_{15} = \frac{(40)^2}{(15.4)^2} \ I_{40} \qquad ,$$

where I_{15} is the spectral radiance in $\mu w/cm^2 \cdot 10\mathring{A}$ at 15.4 cm. In order to determine the sensitivity of the monochromator – PM tube, the observed current output of the PM tube for the standard lamp at a specific wavelength is divided by I_{15}, calculated for the same wavelength, the area of illumination of the photocathode and the bandpass of the monochromator.

To determine the power output of the Xenon Lamp, the observed current output of the PM tube, at a specific wavelength, is divided by the sensitivity of the monochromator – PM tube at the same wavelength. Figure 25 shows the power of the Xenon Lamp incident at the sample site as a function of wavelength.

Nelson showed that the photocurrent in LiF is directly proportional to the intensity of the incident light.[22] From Appendix II, Equation 3, it was shown that

$$N = \frac{P}{A} \ \frac{1}{E}$$

95

FIGURE 25

Power output of the Xenon Lamp incident on the front surface of
the sample
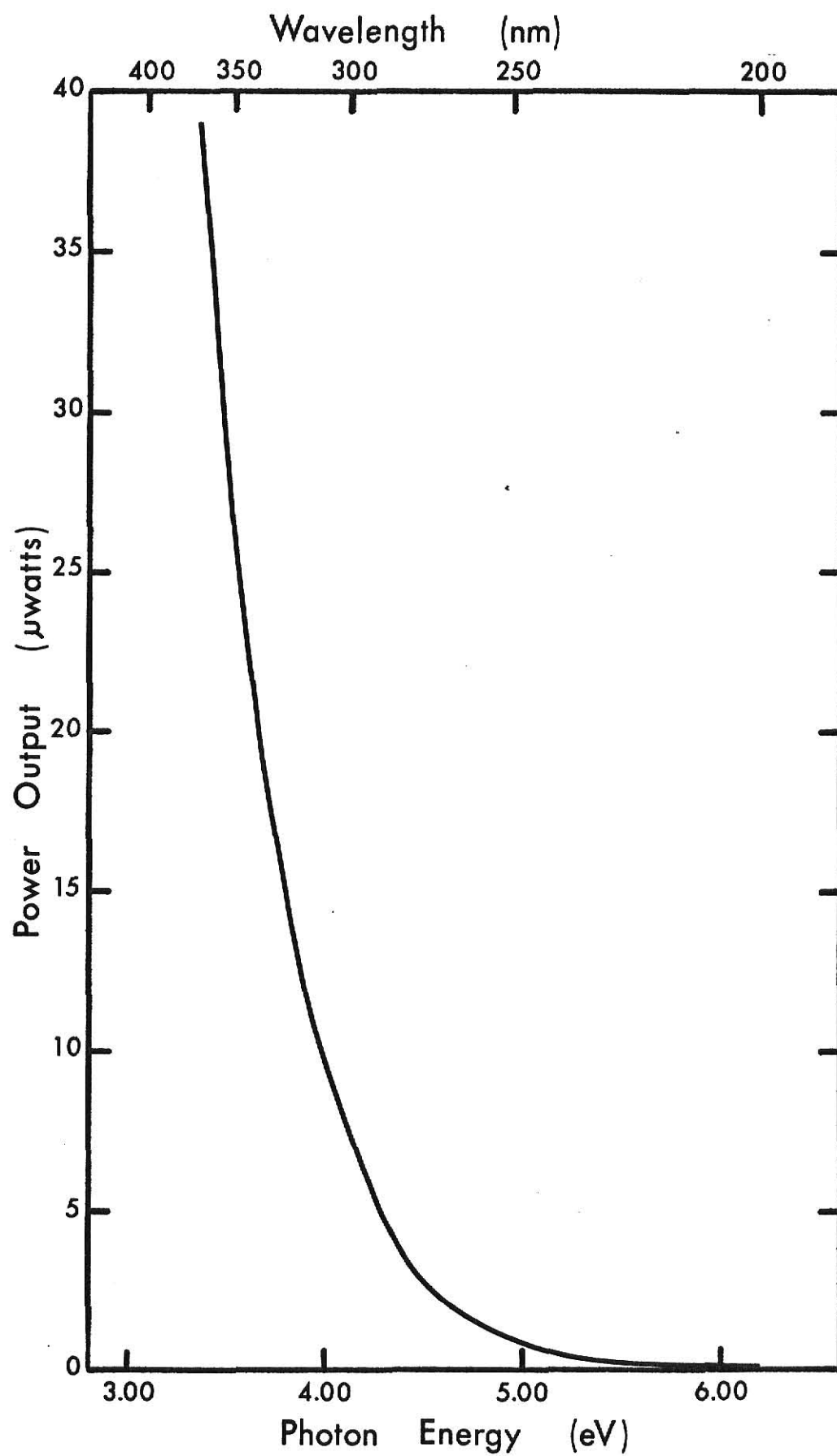
where N is the photon flux at a specific wavelength, P is the power of
the incident light at the same wavelength, A is the area of illumination
and E is the energy of a single photon of the specified wavelength. From
this equation the photon flux is determined for a specified wavelength
and the corresponding photocurrent. The photocurrent is then normalized,
by a proportion, to a photon flux of 9.87×10^{13} photons/cm^2 sec at 370 nm
by

$$\frac{N_1}{i_1} = \frac{N_2}{i_2} \quad ,$$

where N_1 is the photon flux of the Xenon lamp at the sample site, i_1 is the
experimentally observed photocurrent, N_2 is 9.87×10^{13} photons/cm^2 and i_2
is the normalized photocurrent.

A STUDY OF THE OPTICAL ABSORPTION AND PHOTOCONDUCTIVITY

- OF GAMMA-IRRADIATED LiF

by

Charles Denton Marrs

B.S., Fort Hays Kansas State College, 1973

_____

An Abstract of A Master's Thesis

submitted in partial fulfillment of the

requirements for the degree

MASTER OF SCIENCE

Department of Physics

Kansas State University
Manhattan, Kansas

1976

ABSTRACT

The optical absorption and photoconductivity of gamma-irradiated
LiF is studied with emphasis on an unresolved absorption band on the low
energy side ($\sim$4.4 eV) of the F center absorption band (5.0 eV). Response
of the unresolved absorption band, labeled the Y center absorption band,
to [011] and [0$\bar{1}$1] polarized light is examined. The Y center absorption
band is found to be dichroic with respect to these two polarizations of
light. Possible causes of the dichroism are examined and discussed.
The optical bleaching behavior of the Y center absorption band is also
examined. Photoconductivity is observed from the Y center at temperatures
from 85°K to 300°K. The photoconductivity is discussed in terms of the
fundamental processes in a photoconductor and the characteristic relations
of photoconductivity. Using observations from the optical absorption
study and photoconductivity study, a model is proposed for the structure
of the Y center.